P515069.PDF [Page: 3 of 48]

Copy No. 10

DEFENCE R&D DÉFENSE

# ANALYSIS OF VERTICAL NOISE COHERENCE DATA FROM THE EC-VNCI DATA SET

*C. Weatherbee*

*Dalhousie University, Department of Oceanography*

DEFENCE RESEARCH ESTABLISHMENT ATLANTIC

Contractor Report

DREA CR 2000-030

March 2000

National Defence Défense nationale

Canada

THIS IS AN UNEDITED REPORT ON SCIENTIFIC OR TECHNICAL WORK CONTRACTED BY THE DEFENCE RESEARCH ESTABLISHMENT ATLANTIC OF THE RESEARCH AND DEVELOPMENT BRANCH OF THE DEPARTMENT OF NATIONAL DEFENCE, CANADA.

THE CONTENTS OF THE REPORT ARE THE RESPONSIBILITY OF THE CONTRACTOR, AND DO NOT NECESSARILY REFLECT THE OFFICIAL POLICIES OF THE DEPARTMENT OF NATIONAL DEFENCE.

PLEASE DIRECT ENQUIRIES TO:

THE DIRECTOR GENERAL
DEFENCE RESEARCH ESTABLISHMENT ATLANTIC
P.O. BOX 1012
DARTMOUTH, NOVA SCOTIA, CANADA
B2Y 3Z7

P515069.PDF [Page: 5 of 48]

102-02561/

National Defence
Research and Development Branch

Défense nationale
Bureau de recherche et développement

DREA CR 2000-030

# ANALYSIS OF VERTICAL NOISE COHERENCE DATA FROM THE EC-VNCI DATA SET

Cory Weatherbee

Dalhousie University
Department of Oceanography
Halifax, NS, Canada
B3H 4J1

Scientific Authority F. Desharnais

W7707-9-6918/001/HAL
Contract Number

March 2000

CONTRACTOR REPORT

Prepared for

Defence Research Establishment Atlantic

Centre de Recherches pour la Défense Atlantique

Canada

## ABSTRACT

In a shallow water environment, some physical properties of the surficial sediments, such as the compressional and shear speed, can be derived from ambient noise data. Vertical noise coherence data were collected over five sites on the Scotian Shelf and Laurentian Channel. The sites were chosen because of their various sediment properties, in order to quantify whether the differences in vertical coherence would allow differentiation among sediment types. It was found that some sediment types could be differentiated using either the real or imaginary part of the vertical noise coherence (e.g. Sable Island gravel from LaHave clay), while others showed coherence results that were too similar to be differentiated using this technique (e.g. Scotian Shelf drift and LaHave clay). Sites with shipping noise contamination can be difficult to classify.

## RÉSUMÉ

Dans un environnement d'eau peu profonde, les propriétés physiques des sédiments de surface, telles les vitesses d'onde de compression et d'onde transversale, peuvent être inverties du bruit ambiant. La cohérence verticale du bruit ambiant a été mesurée à cinq sites différents sur le plateau continental de la Nouvelle-Écosse et dans le Canal Laurentien. Les sites ont été choisis en fonction des propriétés différentes de leurs sédiments, de façon à déterminer quantitativement si les différences mesurées dans la cohérence verticale permettent de différencier les divers types de sédiment. Il est conclut que certains types de sédiment peuvent être différenciés en utilisant la partie réelle ou la partie imaginaire de la cohérence verticale du bruit ambiant (ex. le gravier de Sable Island et l'argile de LaHave), alors que d'autres types de sédiment produisent des profils de cohérence trop similaires pour être différenciés à l'aide de cette technique (ex. le diluvium du plateau continental et l'argile de LaHave). Les sites qui sont contaminés par du bruit de trafic maritime sont difficiles à classifier.

## TABLE OF CONTENTS


| Section | Page |
|---|---|
| Abstract | i |
| Résumé | i |
| Table of contents | ii |
| 1. Introduction | 1 |
| 2. Experimental set-up | 1 |
| 3. Data processing | 4 |
| 4. Data analysis | 5 |
| 4.1 Data quality | 5 |
| 4.2 Data analysis | 8 |
| 4.2.1 Within site comparison | 10 |
| 4.2.2 Between sites comparison | 10 |
| 5. Conclusions | 11 |
| References | 12 |
| Appendix 1 | 13 |
| Appendix 2 | 14 |
| Appendix 3 | 15 |
| Appendix 4 | 22 |
| Appendix 5 | 29 |
| Appendix 6 | 34 |

## 1. INTRODUCTION

With current sonar technology, the seabed is an important factor in characterising sonar performance [1]. It is therefore beneficial to know as much as possible about a particular seabed when sonar readings are being taken. The seabed, however, is difficult to sample directly. The vertical directionality and coherence of the background noise field are related to the surficial seabed properties [2-4]. Vertical coherence is the normalised cross-correlation of the signal between two vertically separated sensors. The measurement is relatively easy to make, allowing a rapid, though coarse and indirect, measurement of surficial seabed properties.

An experiment was designed to collect vertical noise coherence data over five different sites on the Scotian Shelf and Laurentian Channel. Data from the five sites were compared to determine the overall sensitivity of the coherence technique. If one method is sufficiently sensitive, the data from the different sites could be compared with model results to derive sediment properties.

This report consists of the analysis of the Eastern Canada Vertical Noise Coherence Investigation (EC-VNCI) data set. The aim is to study the effect that different types of seabeds found in the Scotian Shelf and Laurentian Channel have on the vertical coherence of the ambient noise field. The experimental set-up is detailed in the next section, followed by descriptions of data processing and data analysis undertaken, leading to general conclusions about the sensitivity of the technique for the seabed sampled.

## 2. EXPERIMENTAL SET-UP

The Eastern Canada Vertical Noise Coherence Investigation (EC-VNCI) was conducted on December 2nd, 1998. Sonobuoys were deployed and monitored via a Maritime Patrol Aircraft (MPA) over five sites in the Scotian Shelf and Laurentian Channel (see Fig. 1). At each site, nine sonobuoys, in groups of three, were deployed in a triangle pattern (see Fig. 2). Three sonobuoys (AQS-53D(2), AQS-57B and modified AQS-525A) were placed at each apex of the triangle, separated by a distance of ten nautical miles (~18.5 km). An air-deployed expendable bathythermograph (AXBT) was also dropped at the North apex of each site. Only the data from the modified 525A sonobuoys were used for this report. Each 525 sonobuoy has four omnidirectional sensors, but signals from only two were transmitted back to the aircraft. This was done without inter-processing of the channels. The sensors were vertically separated by 3 feet (0.91 m). Data were collected for approximately one hour at each site.

The five sites were chosen for the different sediment types at each location. The site locations and a description of the sediment type at each site are listed in Table 1. The range of compressional sound speed and density expected for each type of sediment was taken from [6].

It should be mentioned that some variation in sediment properties could be expected within some of the sites, as the 10 n. mi. separation between the apices is enough to encompass a change in surficial sediments. At the South East of Halifax site, the sediment type at the East apex is expected to be closer to Scotian Shelf drift than to the mixture of sand and gravel observed at the two other apices [5]. At the Emerald Basin site, the East apex is also closer to Scotian Shelf drift than to LaHave clay [5].

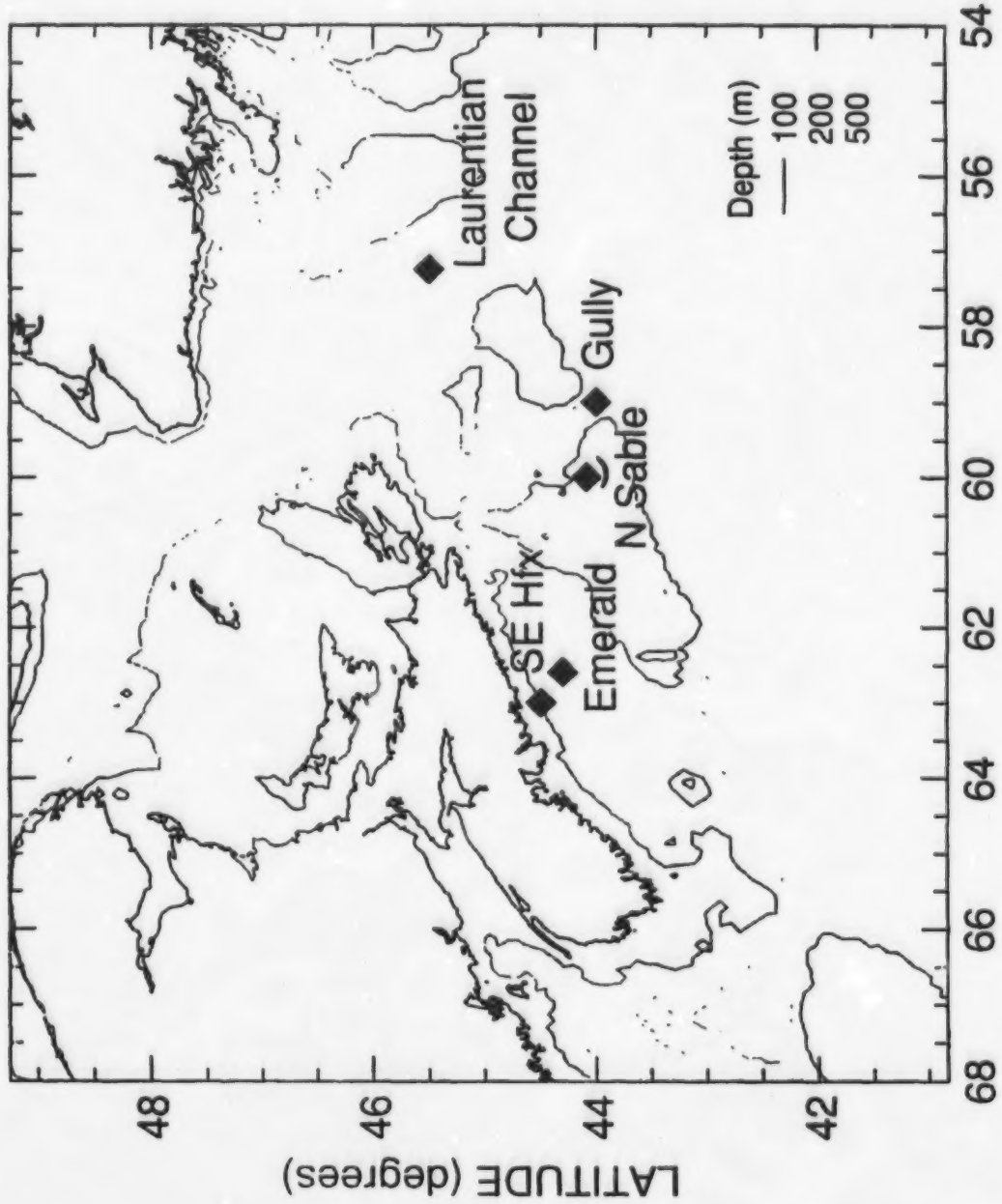


Figure 1. Five EC-VNCI sites off Nova Scotia.

Figure 2. Local sensor deployment for each site.

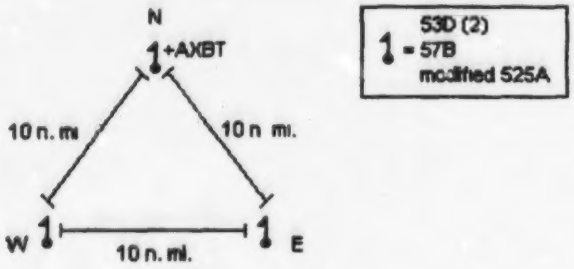


Table 1. Site locations and sediment type at each site. $V_p$ is the compressional sound speed (km/s) and ρ is the density (kg/m$^3$).

| Site | Latitude | Longitude | Sediment Type | Sediment Properties [6] |
|---|---|---|---|---|
| South East of Halifax (North and West apices) | 44° 37' N<br>44° 26' N | 63° 00' W<br>63° 07' W | Sable Island gravel with less than 50% sand [5]. Well-sorted and well-rounded particles. | $V_p$ = 1.67 to 1.9<br>ρ = 2.06 (gravel) |
| North of Sable Island | 44° 09.9' N<br>44° 01.2' N<br>44° 01.3' N | 59° 59.7' W<br>59° 52.8' W<br>60° 06.7' W | Sable Island sand with less than 50% gravel [5]. Well-sorted and well-rounded particles. | $V_p$ = 1.55 to 1.775<br>ρ = 1.7 to 1.96 (sand) |
| Gully | 44° 06.5' N<br>43° 55.9' N<br>43° 55.9' N | 58° 56.7' W<br>58° 52.2' W<br>59° 06.3' W | Sambro sand [6]. Thin veneer (less than 0.3 m) overlying Emerald silt and Scotian Shelf drift formations. | $V_p$ = 1.59 to 1.65<br>ρ = 1.96 |
| Laurentian Channel (all apices) and Emerald Basin (North and West apices) | 45° 35.0' N<br>45° 26.3' N<br>45° 26.4' N<br>44° 22.9' N<br>44° 14.5' N | 57° 24.7' W<br>57° 21.7' W<br>57° 07.6' W<br>62° 35.7' W<br>62° 42.4' W | LaHave clay [6]. Loosely compacted silty clay to clayey silt. | $V_p$ = 1.261 to 1.49<br>ρ = 1.5 to 1.54 |
| East apex of South East of Halifax site, East apex of Emerald Basin (unconfirmed) | 44° 25' N<br>44° 14.5' N | 62° 53' W<br>62° 29' W | Scotian Shelf drift [6]. Cohesive, poorly sorted sediment. Dominantly sandy, but contains silt and clay. | $V_p$ = 1.5 to 1.6 or 1.745 to 1.92, depending on area.<br>ρ = 2.1 |

An air survey was performed to determine the shipping density in a 90-140 km (50 – 75 n. mi.) radius area around each site. Traffic at the South East of Halifax and in the Emerald Basin sites was high (eight ships in a small area around the two sites) since both sites are located at the entrance to Halifax Harbour. A plot of this survey can be found in Appendix 1. The sites North of Sable Island and Gully showed less traffic, with 11 ships distributed over a much larger area (see Appendix 2), and the survey of the Laurentian Channel site found no ships within 140 km.

## 3. DATA PROCESSING

The original analogue data were stored on magnetic tape and digitised onto DLTs (Digital Linear Tapes) using the Acoustic Data Replay Facility (ADRF) at DREA. The data were digitized at a rate of 6554 Hz. PRODAT (signal processing software proprietary to DREA) was used to process the time series. PRODAT was run on an AXP computer with VMS 7.1 operating system. The processed files were then transferred to a SIDUS Pentium 133 MHz computer (running Microsoft Windows 95) for subsequent analysis.

The vertical coherence analysis is the normalized cross-correlation between the two vertically-separated omnidirectional channels of each modified 525A sonobuoy, represented in the frequency domain as:

$$\Gamma_{12} = \frac{\overline{S_{12}}}{\sqrt{\overline{S_{11}}\,\overline{S_{22}}}}, \qquad (1)$$

where $\overline{S_{11}}$ and $\overline{S_{22}}$ are the average auto-spectra of the two channels, and $\overline{S_{12}}$ is the average cross-spectrum. PRODAT calculated $\Gamma_{12}$ using the following settings:

- time average of one minute, with no overlap between records,
- 4096 points per FFT period,
- "Hanning" window type,
- mean of the data removed, so that the data would be centred at zero, and
- cross-spectra given, as well as auto-spectra, to allow for the calculation of vertical coherence.

Table 2 lists the two channel numbers (in the DREA ".dat" file with the digitized time series) of all three 525A sonobuoys of each site. The vertical noise coherence of each site was saved in a DREA ".coh" file for further analysis.

Table 2. Channel numbers in the DREA ".dat" file (digitized time series) and DREA ".coh" files (processed coherence data) for the sonobuoys of each site.

| Site | Apex | Channel numbers in DREA ".dat" files | Channel numbers in DREA ".coh" files |
|---|---|---|---|
| South East of Halifax | North | 9, 25 | 0 |
| | West | 2, 18 | 1 |
| | East | 10, 26 | 2 |
| Emerald Basin | North | 9, 25 | 0 |
| | West | 2, 18 | 1 |
| | East | 10, 26 | 2 |
| North of Sable Island | North | 9, 25 | 0 |
| | East | 2, 18 | 1 |
| | West | 10, 26 | 2 |
| Gully | North A | 9, 25 | 0 |
| | North B | 16, 32 | 1 |
| | East | 2, 18 | 2 |
| | West | 10, 26 | 3 |
| Laurentian Channel | North | 10, 26 | 0 |
| | West | 9, 25 | 1 |
| | East | 2, 18 | 2 |

## 4. DATA ANALYSIS

### *4.1 Data Quality*

Quality checks were made on all data records to eliminate periods of "bad" or noise contaminated data. Bad data could result from a number of factors: a ship passing by the sonobuoy, a malfunctioning hydrophone, or a sonobuoy still descending to depth (so that flow noise artificially increased the noise level), or any contamination from other coherent sources. Malfunctioning hydrophones or hydrophones affected by flow noise were identified by plotting the individual spectra as a function of time for several frequency bands. Periods affected by shipping noise, or other broadband noise contamination, were identified by plotting the real and imaginary coherence as a function of frequency and time, and by looking for suspicious behaviour, such as increased levels in the real part (see [7] for the effect of shipping noise on vertical coherence). Table 3 lists the site, apex, record combinations that were categorized as good or uncontaminated data in both the real and imaginary parts. A record represents an averaging period of 1 minute.

Table 3. Good site, apex, record combinations.

| Site | Apex | Good Records in Coherence Data (both real and imaginary parts) | Number of Good Records |
|---|---|---|---|
| South East of Halifax | North | 20-31, 59-61, 71-73 | 18 |
| | West | 36-51 | 16 |
| | East | 13-15, 17-26, 29-47, 49-70 | 54 |
| Emerald Basin | North | 5-6, 8-9, 13, 19-20, 30-37, 57-60, 62-65 | 23 |
| | West | 5-33, 35-62 | 57 |
| | East | 6-13, 16-33, 37-46, 49-54, 57-58, 60, 62 | 46 |
| North of Sable Island | North | 2-72 | 71 |
| | East | None | 0 |
| | West | 9-71 | 63 |
| Gully | North A | 17-73 | 57 |
| | North B | None | 0 |
| | East | 6-73 | 68 |
| | West | 29-33, 35, 40-41, 44-45, 49-50, 56-59, 67-71 | 21 |
| Laurentian Channel | North | 15-74 | 60 |
| | West | 6-70 | 65 |
| | East | None | 0 |

The individual plots of coherence as a function of frequency (for the records listed in Table 3) are included as grey curves in Appendix 3 (real part) and Appendix 4 (imaginary part) for each site. The average of these data (averaged over all the records) is over-plotted in black. Table 4 compiles some observations that were made upon inspection of these data plots.

Table 4. Notes on data quality.

| Site | Apex | Notes |
|---|---|---|
| South East of Halifax | North | There was an unidentified spike at approximately 1200 Hz (real coherence) throughout most records.<br>Several records had low coherence (real part) below 500 Hz, indicating that a significant amount of noise is coming from coherent sources in the area. There were several CW lines as well (as expected in a high shipping area). |
| | West | There was a strong line in the real coherence near 1100 Hz, and unidentified noise in the 800 – 1000 Hz band. Fewer shipping lines than at the North apex. |
| | East | For frequencies greater than about 800 Hz, the real coherence data were low relative to other apices. The imaginary part is also different for the East apex (larger amplitude of oscillations). The difference between East and the other two apices may be due to a difference in surficial sediment type. |
| Emerald Basin | North and West | Real coherence at both apices are relatively close to one another, except in the 700 to 1200 Hz band, where shipping noise is higher for the North apex. The imaginary parts are also similar, except below 300 Hz (more noise on West apex). |
| | East | The real coherence at this apex was not consistent with the other apices in the Emerald Basin site. The difference may be due to a difference in surficial sediment type. The second positive peak, near 2000 Hz, was lower in this apex.<br>The amplitudes of the oscillations in the imaginary part were low relative to the other apices in the Emerald Basin site. |
| North of Sable Island | North and West | Data of both apices (North and West) appear good, but the real part of the North apex is significantly lower than that of the West apex and is not centred at zero. The imaginary part of the West apex has lower amplitude oscillations. |
| | East | Sonobuoy was not functioning properly. Data are not valid. |
| Gully | North B | The first sonobuoy dropped at this apex was not functioning (North B in Table 2), and was replaced by a second sonobuoy (North A) during the flight. |
| | North A, East, West | Agreement for all three apices was excellent, in both the real and imaginary parts. |
| Laurentian Channel | East | One of the sensors from this sonobuoy was not functioning properly. Coherence data are not valid. |
| | North and West | Agreement for both apices is very good, in both the real and imaginary parts. |

*4.2 Data Analysis*

The goal of this section is to compare the real and imaginary coherence of the various apices and sites, and see if there are significant differences based on presumed seabed types. To facilitate this comparison, it was necessary to smooth the mean coherence curves (both real and imaginary parts) from Appendices 3 and 4 (black curves). A curve-fitting algorithm was applied to these curves, but it was found that a running average produced better results.

The n-point running average was defined for each frequency bin as the average of not only the records in that frequency bin, but also the records in the next n-1 frequency bins. Thus, the first point in the n-point running average was the average of all records from frequency bins zero to n-1. The second point was the average from 1 to n, and so on. An 11-point running average (corresponding to a frequency band of 17.6 Hz) was found to smooth the coherence curves reasonably well, without visibly affecting the inflexion points.

The sum of the squared differences (SSDs) between smoothed coherence curves was used to quantify the degree of similarity or difference between apices and sites. For the real coherence data, this statistic was calculated for frequencies between 320 and 3200 Hz. This frequency range was chosen to eliminate the effect of the high variation that occurred below 320 Hz and above 3200 Hz. For imaginary data the SSD was calculated over all frequencies. Table 5 shows the SSD data for all pairs of apices for the real coherence data, and Table 6 shows the same information for the imaginary coherence data.

Table 5. Sum of squared differences data for 11-point running average between 320 and 3200 Hz (real coherence).

| | | South East of Halifax | | Emerald Basin | | | North of Sable Is. | | Gully | | | Laurentian Channel | |
|---|---|---|---|---|---|---|---|---|---|---|---|---|---|
| | | W | *E* | N | W | *E* | N | W | N A | E | W | N | W |
| South East of Halifax | N | 8 4 | *27.2* | **9.9** | 19.0 | *36.0* | 65.1 | **13.9** | 27.8 | **26.0** | 28 7 | **28.5** | 33.1 |
| | W | - | *28.7* | 10.8 | 23.4 | *35.2* | 60.1 | 14 7 | 25.8 | 22.1 | 25.2 | 27.9 | 36.5 |
| | *E* | - | - | *11.5* | *8.9* | *5.8* | *13.0* | *7.3* | *7.5* | *7 1* | *6.2* | *3.4* | *5.8* |
| Emerald Basin | N | - | - | - | 4.7 | *20 7* | 39.9 | **8.9** | 13.7 | **10.9** | 13.9 | **11.4** | 16 8 |
| | W | - | - | - | - | *23.6* | 39.1 | 15.7 | 19.1 | 16.2 | 18 9 | 12.8 | 17.5 |
| | *E* | - | - | - | - | - | *5.2* | *6.3* | *2.4* | *3.8* | *1.7* | *3.0* | *3.2* |
| North of Sable Island | N | - | - | - | - | - | - | 21.8 | 12.0 | 13.6 | 9.8 | 11.3 | 11.7 |
| | W | - | - | - | - | - | - | - | 3.8 | **4.0** | 3.8 | **5.2** | 7.0 |
| Gully | N A | - | - | - | - | - | - | - | - | 0.5 | 0 6 | 1 5 | 2 4 |
| | E | - | - | - | - | - | - | - | - | - | 0 7 | **1.5** | 3.9 |
| | W | - | - | - | - | - | - | - | - | - | - | 1 7 | 3.6 |
| Laurentian Channel | N | - | - | - | - | - | - | - | - | - | - | - | 1 4 |

Table 6. Sum of squared differences data for 11-point running average (imaginary coherence).

| | | South East of Halifax | | Emerald Basin | | | North of Sable Is. | | Gully | | | Laurentian Channel | |
|---|---|---|---|---|---|---|---|---|---|---|---|---|---|
| | | W | *E* | N | W | *E* | N | W | NA | E | W | N | W |
| South East of Halifax | N | 1.8 | *2.3* | **8.9** | 30.4 | *7.6* | 7.5 | **19.6** | 4.9 | **3.5** | 5.0 | **7.8** | 7.2 |
| | W | - | *6.4* | 10.8 | 33.4 | *13.2* | 13.1 | 28.2 | 9.4 | 6.6 | 9.9 | 11.0 | 12.1 |
| | *E* | - | - | *11.1* | *30.5* | *2.5* | *3.0* | *10.7* | *2.3* | *3.0* | *2.2* | *7.5* | *4.1* |
| Emerald Basin | N | - | - | - | 18.3 | *17.2* | 11.4 | **34.6** | 7.9 | **4.3** | 8.2 | **3.5** | 6.3 |
| | W | - | - | - | - | *28.7* | 22.0 | 36.9 | 20.9 | 19.6 | 20.2 | 14.6 | 19.4 |
| | *E* | - | - | - | - | - | *2.1* | *4.8* | *3.0* | *6.9* | *2.5* | *10.7* | *5.0* |
| North of Sable Island | N | - | - | - | - | - | - | 8.0 | 1.1 | 3.0 | 1.0 | 5.8 | 2.5 |
| | W | - | - | - | - | - | - | - | 11.9 | **17.5** | 10.8 | **23.1** | 15.4 |
| Gully | NA | - | - | - | - | - | - | - | - | 1.8 | 0.4 | 3.0 | 1.1 |
| | E | - | - | - | - | - | - | - | - | - | 2.2 | **2.3** | 2.5 |
| | W | - | - | - | - | - | - | - | - | - | - | 3.9 | 1.5 |
| Laurentian Channel | N | - | - | - | - | - | - | - | - | - | - | - | 1.9 |

A representative apex was selected for each site for the purpose of inter-site comparisons. Table 7 below lists these apices.

Table 7. Representative apex for each site.

| Site | Representative Apex |
|---|---|
| South East of Halifax | North |
| Emerald Basin | North |
| North of Sable Island | West |
| Gully | East |
| Laurentian Channel | North |

The SSD numbers for these representative apices (as defined in Table 7) are in bold fonts in Tables 5 and 6; the numbers in italics are for apices with data of questionable quality (see section 4.2.1). For all combinations of any two of these representative apices, a plot of the apices' 11-point running average was generated (see Appendices 5 and 6).

*4.2.1 Within-Site Comparison*

The site South East of Halifax, which had spikes in the real coherence near 1100 Hz, showed the North apex to be similar to the West apex, but the East apex was different from each of these (see Appendix 3). Although the East apex had the same period as the other apices, the amplitude of oscillations in the real coherence was lower at frequencies above 800 Hz. The same situation prevailed at the Emerald Basin site. The North and West apices were similar, but the East apex did not match either of the other apices because it had lower amplitude on the second local maximum above 900 Hz (see Appendix 3, average real coherence). The imaginary part of the coherence (Appendix 4) was also different for the East apices of these two sites. The differences for these two apices agree with the potential difference in sediment types (see Table 1).

At the North of Sable Island site, which had fairly smooth data, the real coherence data for the two apices were not very similar to one another (see Appendix 3). The oscillations had the same period, but the overall curve at the North apex was lower above 900 Hz. This apex had better data below 500 Hz, but the West apex was a better fit with the other sites. Without data from a third apex, it is difficult to know whether the difference between the North and West apices come from a significant change in sediment type, of from invalid data at one of the apices.

The real and imaginary coherence data for the three apices in the Gully site (see Appendixes 3 and 4) were very smooth and had excellent agreement. Data from the two apices of the Laurentian Channel were also consistent and very smooth in nature (both real and imaginary parts). Neither the Gully site nor the Laurentian Channel site showed contamination from shipping noise.

*4.2.2 Between-Sites Comparison*

The between-sites comparison is complicated by the variable amount of shipping noise for the various sites. Shipping noise contamination increases the average SSD values for a given site due to the additional structure in the curves. For these between-sites comparisons, the sizes of the SSD values across two sites are first compared to the sizes of the SSD values within each site. If the across-site SSD is significantly larger than the within-site SSD values, the assumption is made that the coherence curves (real or imaginary or both) are different enough to allow differentiation between the sites.

Analysing the SSD data (bold values in Tables 5 and 6) for apices in different sites, it was found that the real and imaginary SSD values for the Gully and Laurentian Channel sites are very close, and it is unlikely that the sediment types of these sites (Sambro sand and LaHave clay) could be differentiated using the coherence technique (the SSDs across the sites were comparable to the SSDs within the sites). This suggests that the seabed of the Gully is filled with LaHave clay, which could not be confirmed at the time this report was written, but is not unlikely from a geological point of view.

The real SSD values of the North of Sable Island site (based on the West apex data) were close the values for the Gully and the Laurentian Channel (in the order of five units), and the within-site SSDs were high. Either the data of the North apex in the North of Sable Island site were bad or the sediment type is highly variable at the North of Sable Island site. The imaginary

part, on the contrary, indicates a larger difference between the North of Sable Island site and the Gully and Laurentian Channel sites than within the North of Sable Island site. This indicates that Sable Island sand could be differentiated from LaHave clay, based on the imaginary coherence data.

The imaginary parts of the SSDs between the Emerald Basin site and the Gully and Laurentian Channel sites were low, suggesting that these sites are similar. This agrees with Table 1, which shows that the Emerald Basin site and the Laurentian Channel site are similar. The real parts, however, of the SSDs involving the Emerald Basin site indicate that this site is equally different from all the other sites. This could be due to the poor quality of the real coherence data for this site (high shipping noise and noise in the 700 to 1200 Hz band).

The examination of the between-site SSDs involving the South East of Halifax site (Sable Island gravel) suggests that this site should be differentiable from all the other sites, more so from the LaHave clay from the Laurentian channel if the real part of the coherence is used, though more from the Sable Island sand if the imaginary coherence is considered. The data from the SE of Halifax site, however, was affected by shipping noise, which may decrease the significance of the results.

Finally, the drift from the SE of Halifax and Emerald Basin sites (East apices) are very similar, based on the low SSDs of both the real and imaginary coherence. This sediment type, however, could not be distinguished from the LaHave clay of the Gully and Laurentian Channel.

## 5. CONCLUSIONS

The data collected in the Eastern Canada Vertical Noise Coherence Investigation were analysed first to determine their quality. After this initial testing, the data were analysed to determine whether the coherence was a sensitive-enough statistic to allow differentiation among five sites with different sediments properties. It was found that:

- Sable Island gravel (with less than 50% sand) can be differentiated from the other types of sediments, mostly from the LaHave clay from the Laurentian channel (if the real part of the coherence is used) and from the Sable Island sand (with less than 50% gravel) from North of Sable Island (if the imaginary part of the coherence is used);
- The Sambro sand from the Gully and the LaHave clay from the Laurentian channel could not be differentiated, possibly because the Gully is filled with LaHave clay;
- The Sable Island sand (North of Sable Island) can be differentiated from the LaHave clay using the imaginary part of the coherence (but not the real part);
- The LaHave clay from Emerald Basin can be differentiated from the other sediments (using real coherence), though the imaginary coherence is similar to that of the LaHave clay from the Laurentian channel;
- The Scotian Shelf drift from the East apices of both the SE of Halifax and Emerald Basin sites are similar, and cannot be differentiated from the LaHave clay of the Laurentian channel.

Some of these results might have been affected by shipping noise contamination, particularly for the SE of Halifax site and the Emerald Basin site. In the future, model estimates

of vertical noise coherence using estimated bottom properties will be calculated for these five sites. Data-model comparisons should allow us to determine if shipping noise was an issue in our measurements, and whether accurate sediment parameters, mainly the compressional sound speed, shear speed and density, can successfully be inverted for any of these sites.

## REFERENCES


1. Urick, R. J., "Principals of underwater sound" 3rd ed., McGraw-Hill, 1983.
2. Desharnais, F. and Chapman, D.M.F. "Vertical coherence of the shallow water ambient noise field, a model", DREA Technical Memorandum 1999-011, 1999.
3. Buckingham, M.J. and Jones, S.A.S., "A new shallow-ocean technique for determining the critical angle of the seabed from the vertical directionality of the ambient noise in the water column," J. Acoust. Soc. Am., 1987, **81**, 938-946.
4. Harrison, C.H., "Formulas for ambient noise level and coherence." J. Acoust. Soc. Am., 1996, **99**, 2055-2066.
5. Scotian Shelf Surficial Geology, Halifax to Sable Island. Chart 4040-G published by the Canadian Hydrographic Service, Ottawa, 1970.
6. Osler, J.C., "A geo-acoustic and oceanographic description of several shallow water experimental sites on the Scotian Shelf", DREA Technical Memorandum 94/216, 1994.
7. Desharnais, F., B.R. MacDonald and K.J. Mah, "Vertical Noise Coherence Measurements in Shallow Water Using Lagrangian Drifters," Proceedings of 16th International Congress on Acoustics and 135th Meeting Acoustical Society of America, Seattle, US. Vol. 2, 1998, pp. 981-982.

**Appendix 1.** Shipping survey, South East of Halifax and Emerald Basin.

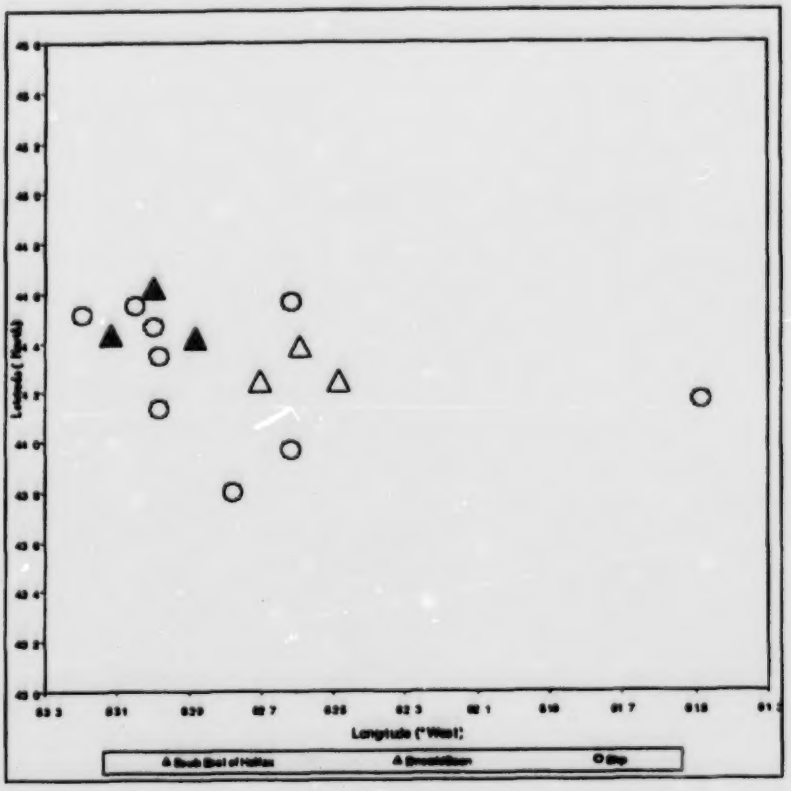

**Figure 1.1.** Shipping survey, South East of Halifax and Emerald Basin. Black triangles represent the 3 apices of the SE of Halifax site, white triangles represent the three apices of the Emerald Basin site, circles represent ships sighted from the aircraft.

**Appendix 2.** Shipping Survey; North of Sable Island and Gully.

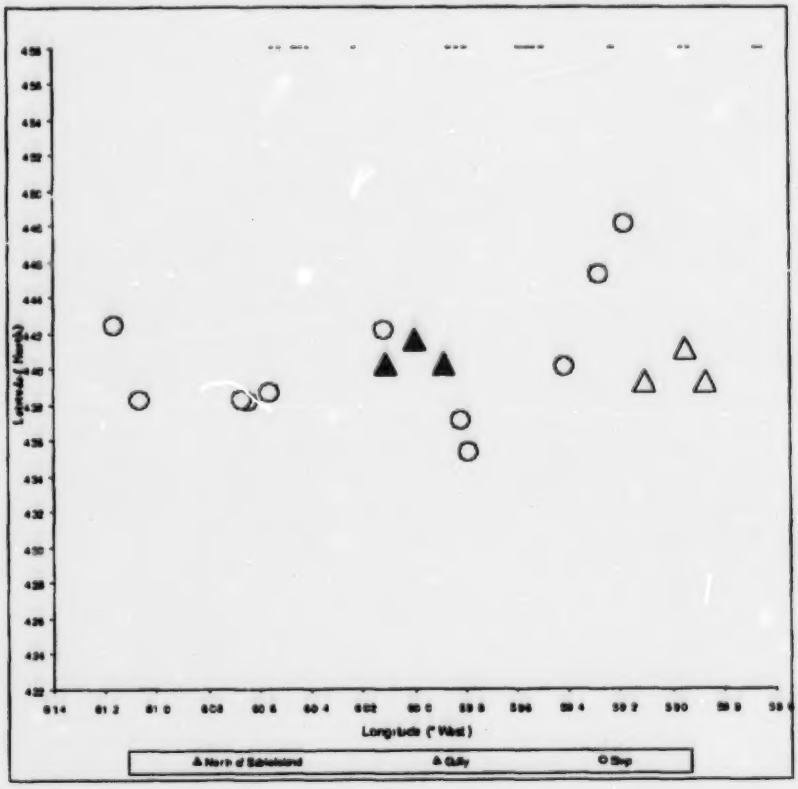

Figure 2.1. Shipping Survey; North of Sable Island and Gully. . Black triangles represent the 3 apices of the North of Sable Island site, white triangles represent the three apices of the Gully site, circles represent ships sighted from the aircraft.

**Appendix 3.** Plots of real coherence data and mean.

Figure 3.1. Plot of real coherence as a function of frequency for the valid data records (grey) and the average data (black). South East of Halifax site, North Apex.

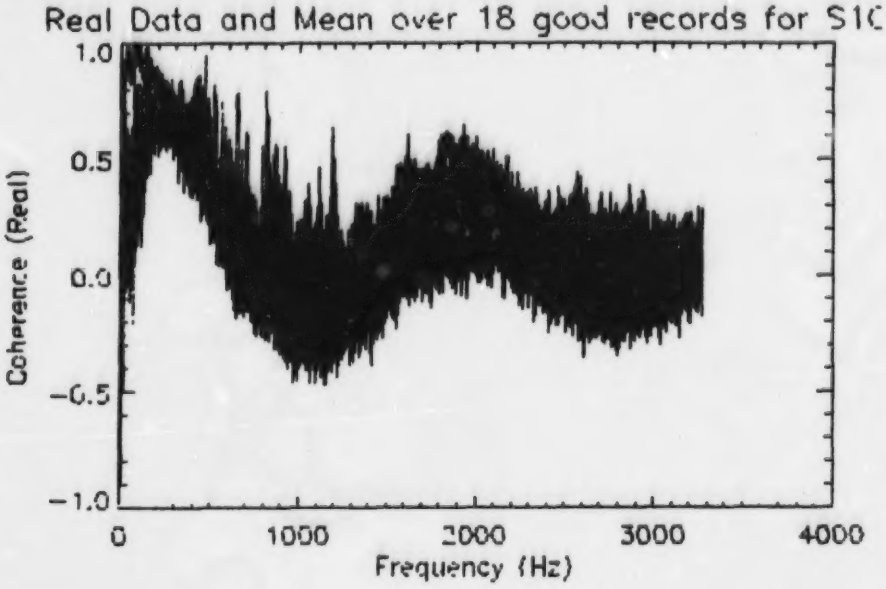


Figure 3.2. Plot of real coherence as a function of frequency for the valid data records (grey) and the average data (black). South East of Halifax site, West Apex.

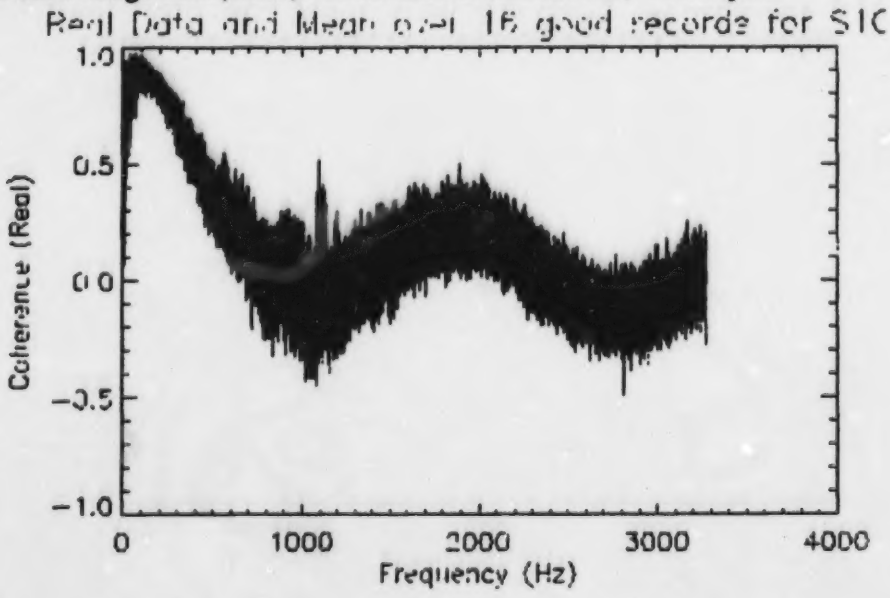

Figure 3.3. Plot of real coherence as a function of frequency for the valid data records (grey) and the average data (black). South East of Halifax site, East Apex.

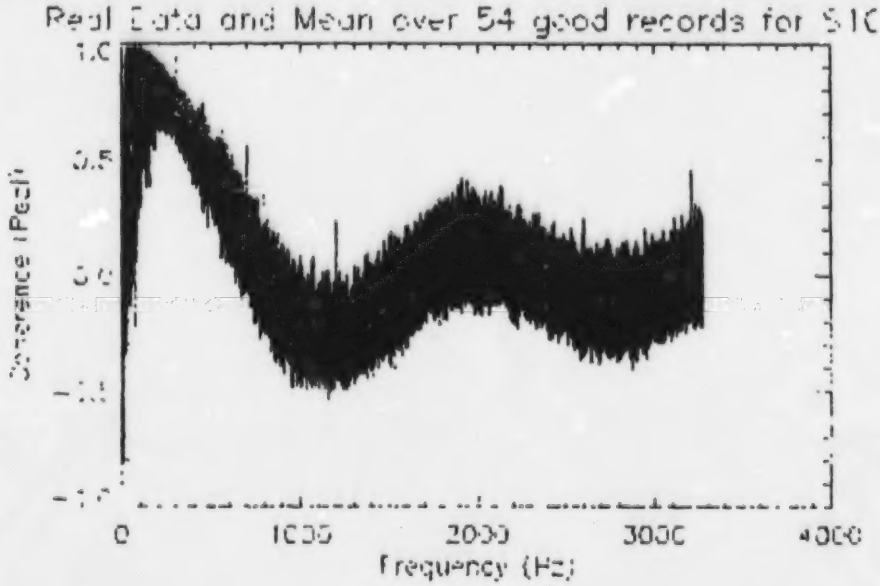


Figure 3.4. Plot of real coherence as a function of frequency for the valid data records (grey) and the average data (black). Emerald Basin site, North Apex.

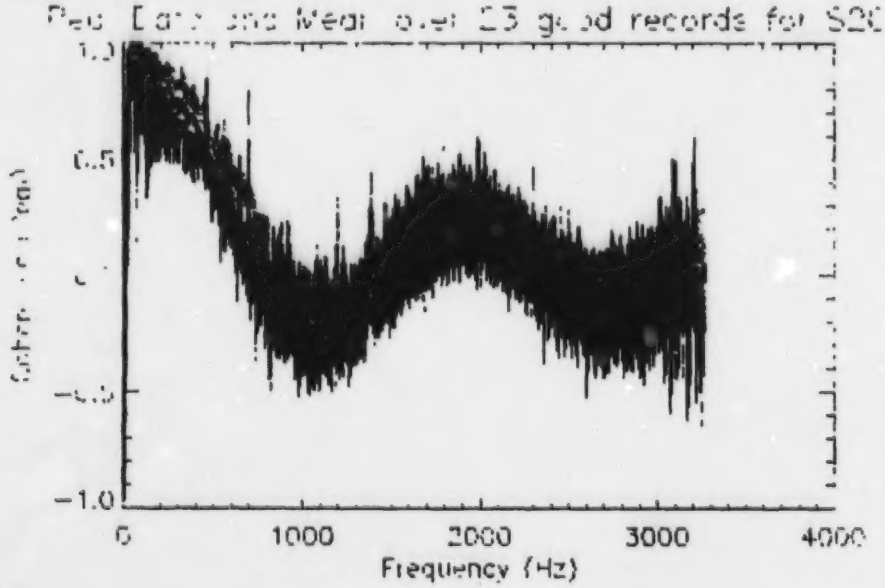

Figure 3.5. Plot of real coherence as a function of frequency for the valid data records (grey) and the average data (black). Emerald Basin site, West Apex.

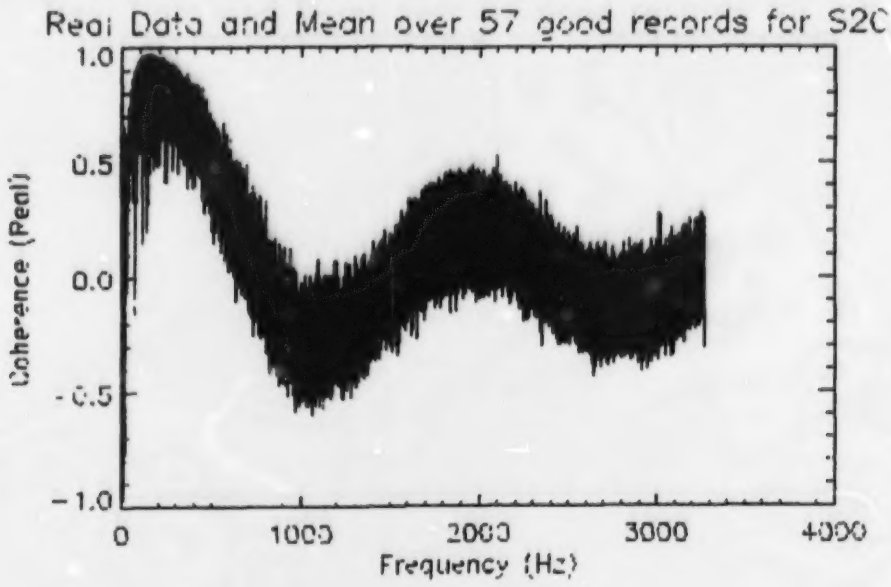


Figure 3.6. Plot of real coherence as a function of frequency for the valid data records (grey) and the average data (black). Emerald Basin site, East Apex.

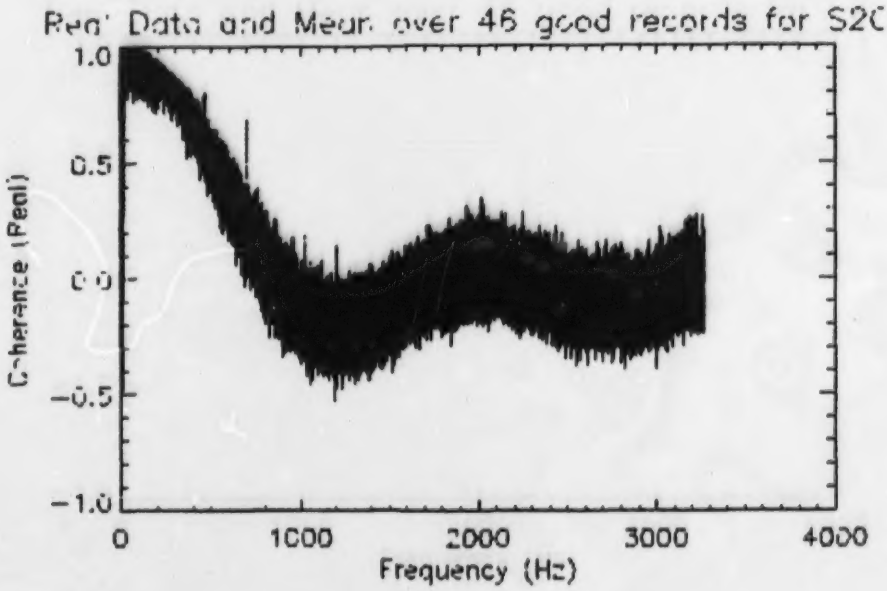

Figure 3.7. Plot of real coherence as a function of frequency for the valid data records (grey) and the average data (black). North of Sable Island site, North Apex.

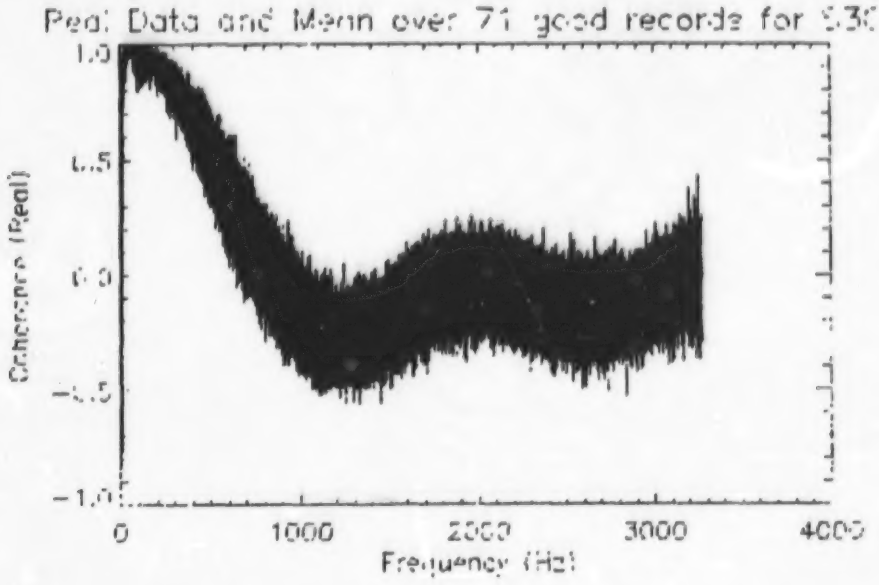


Figure 3.8. Plot of real coherence as a function of frequency for the valid data records (grey) and the average data (black) North of Sable Island site, West Apex.

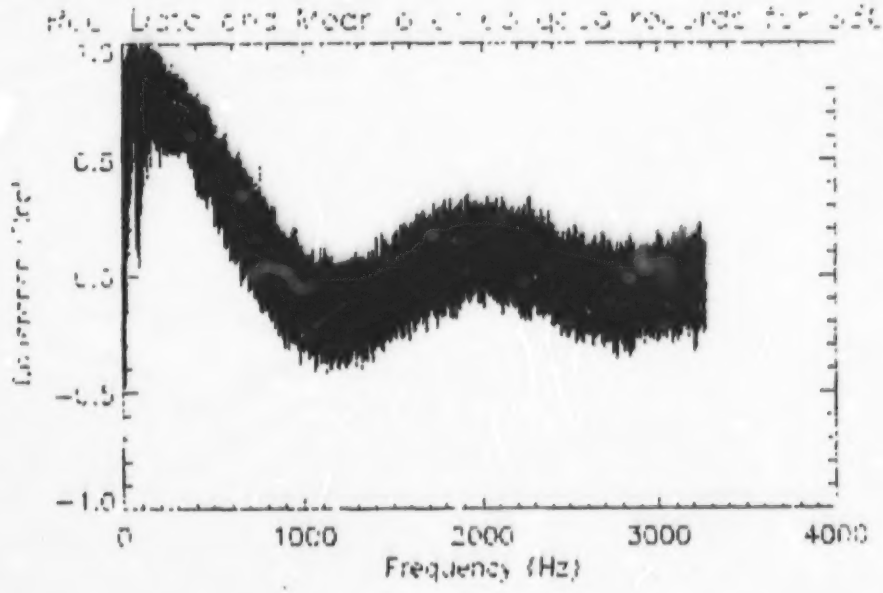

Figure 3.9. Plot of real coherence as a function of frequency for the valid data records (grey) and the average data (black). Gully site, North A Apex.

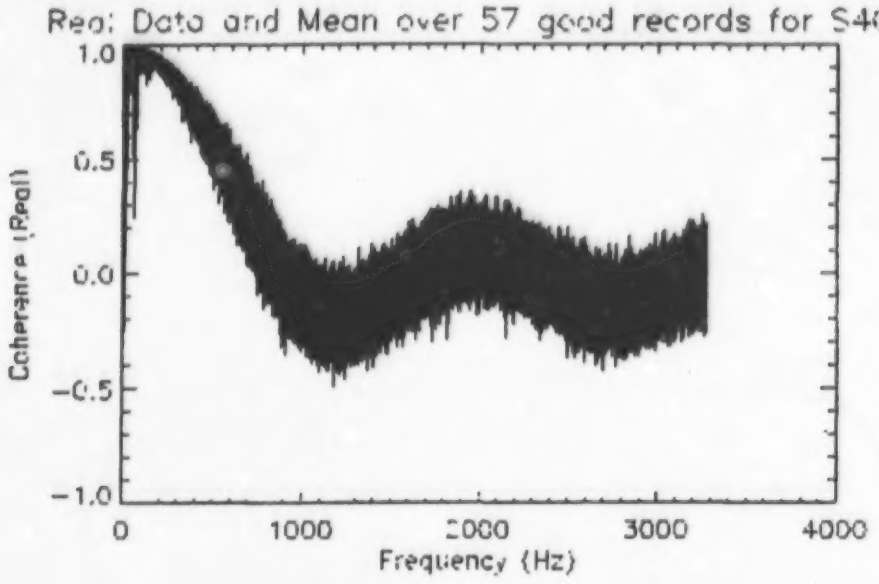


Figure 3.10. Plot of real coherence as a function of frequency for the valid data records (grey) and the average data (black). Gully site, East Apex.

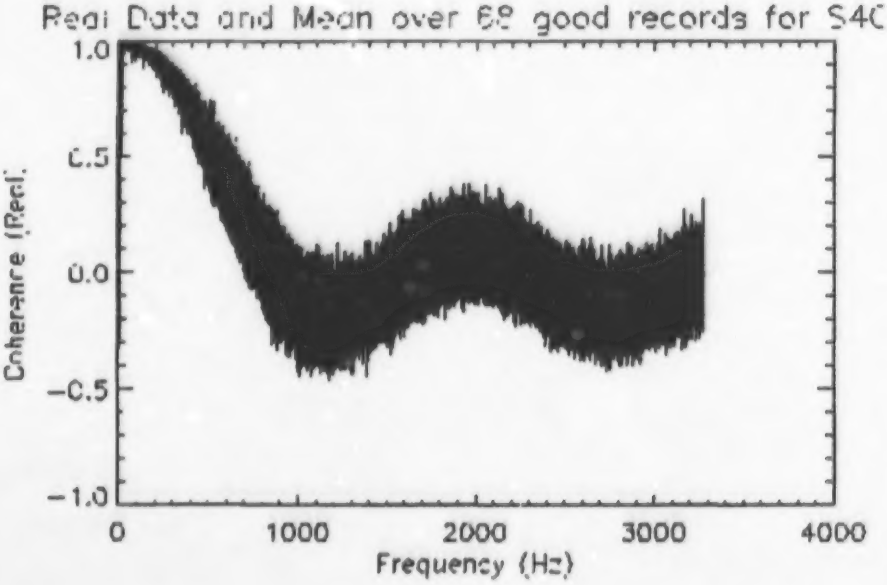

Figure 3.11. Plot of real coherence as a function of frequency for the valid data records (grey) and the average data (black). Gully site, West Apex.

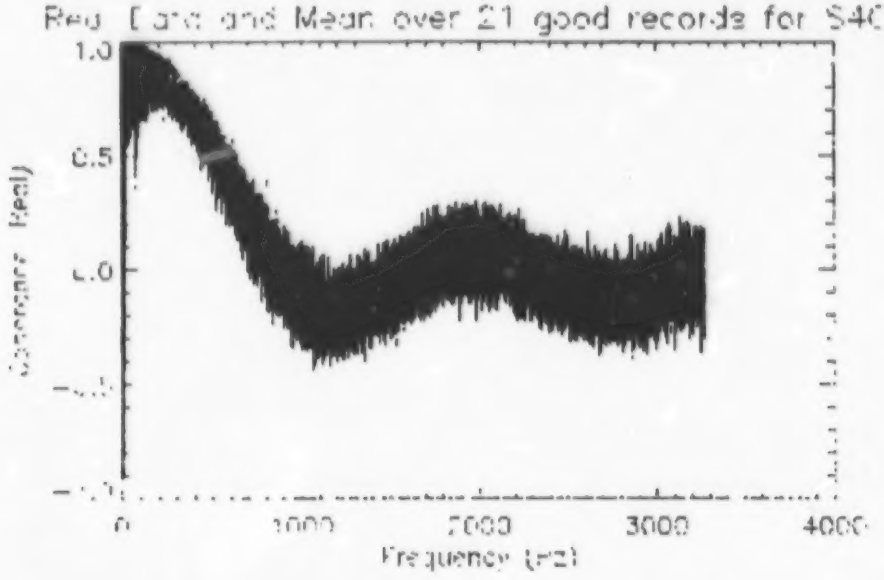


Figure 3.12. Plot of real coherence as a function of frequency for the valid data records (grey) and the average data (black). Laurentian Channel site, North Apex.

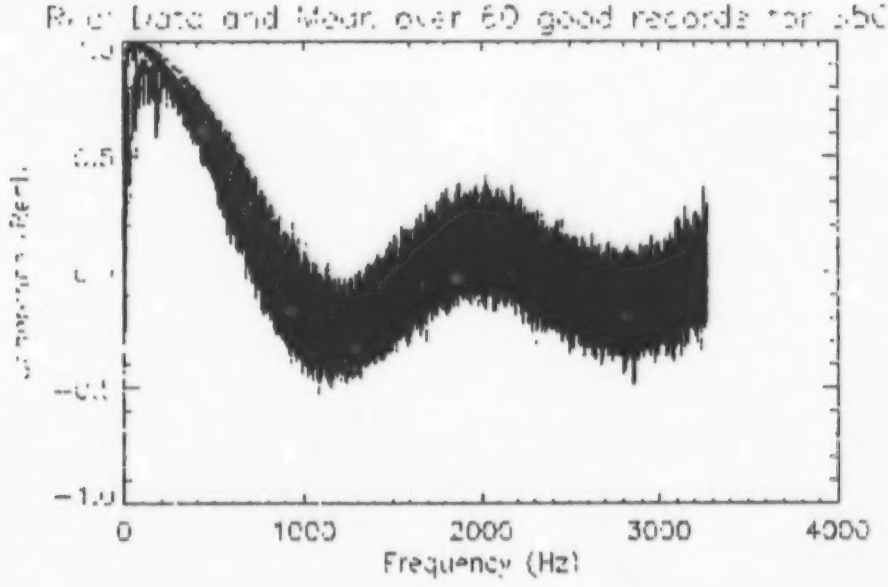

Figure 3.13. Plot of real coherence as a function of frequency for the valid data records (grey) and the average data (black). Laurentian Channel site, West Apex.

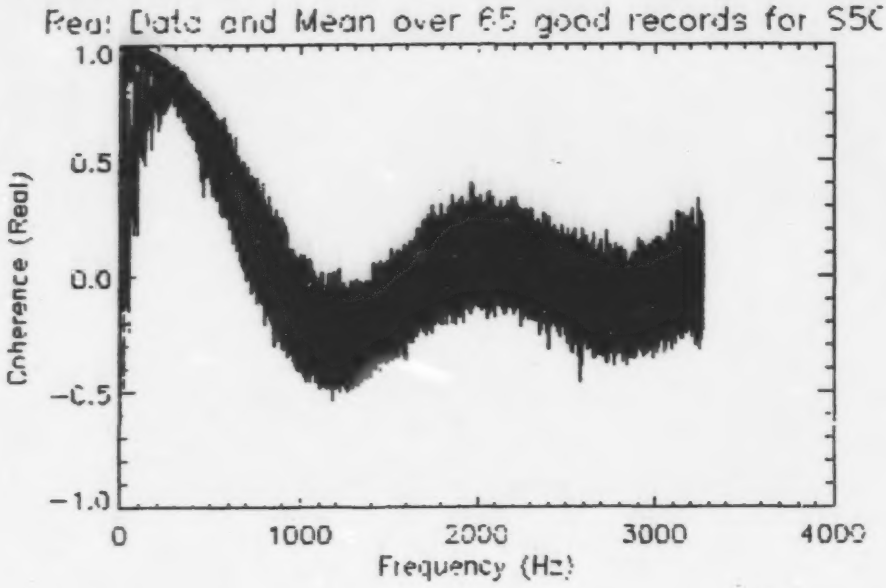

**Appendix 4.** Plots of imaginary coherence data and mean.

Figure 4.1. Plot of imaginary coherence as a function of frequency for the valid data records (grey) and the average data (black). South East of Halifax site, North Apex.

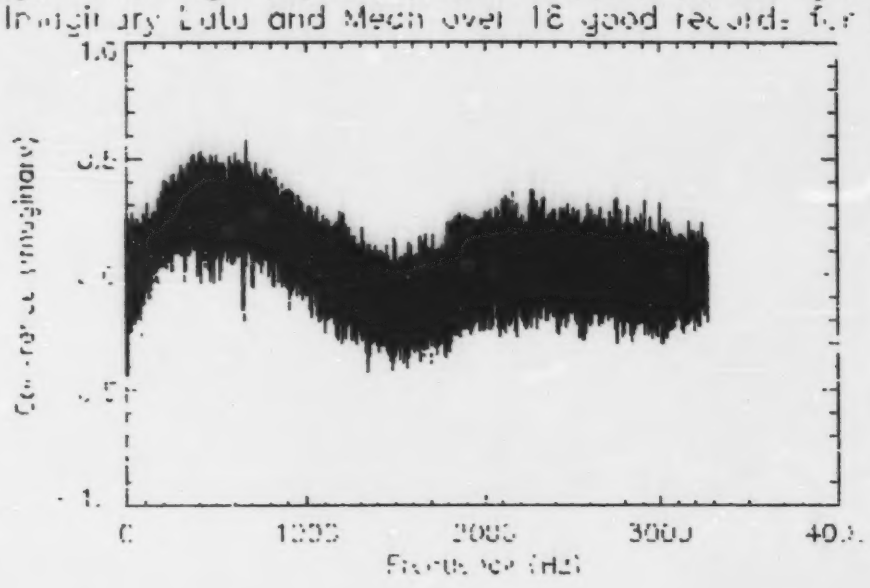


Figure 4.2. Plot of imaginary coherence as a function of frequency for the valid data records (grey) and the average data (black). South East of Halifax site, West Apex.

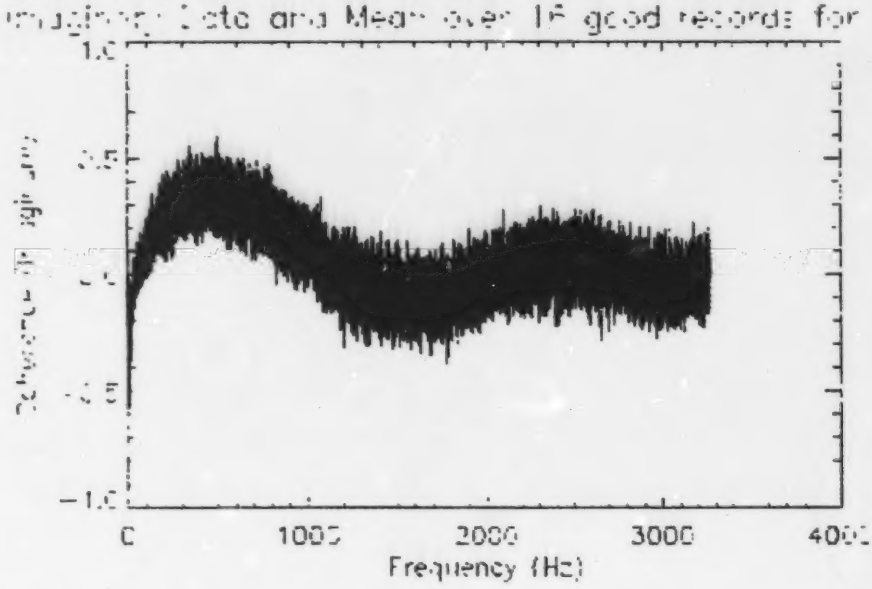

**Figure 4.3. Plot of imaginary coherence as a function of frequency for the valid data records (grey) and the average data (black). South East of Halifax site, East Apex.**

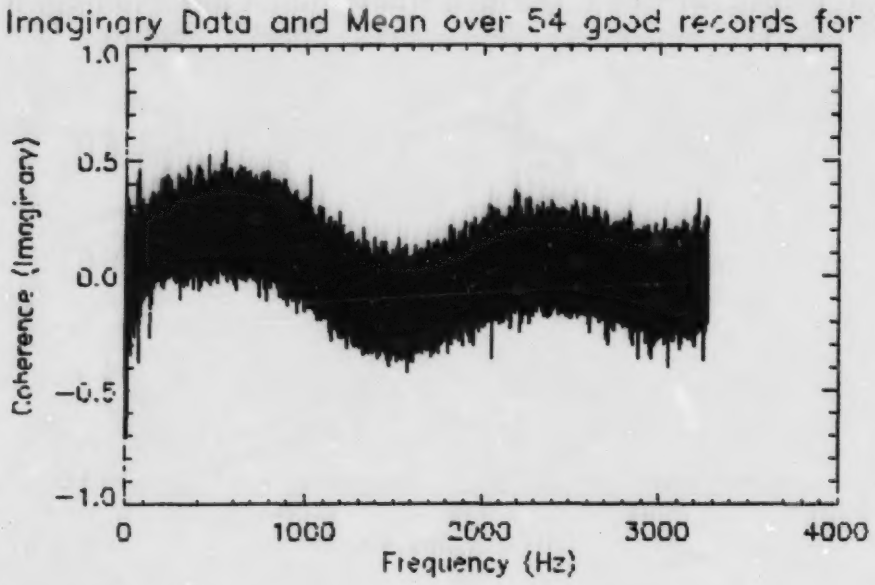


**Figure 4.4. Plot of imaginary coherence as a function of frequency for the valid data records (grey) and the average data (black). Emerald Basin site, North Apex.**

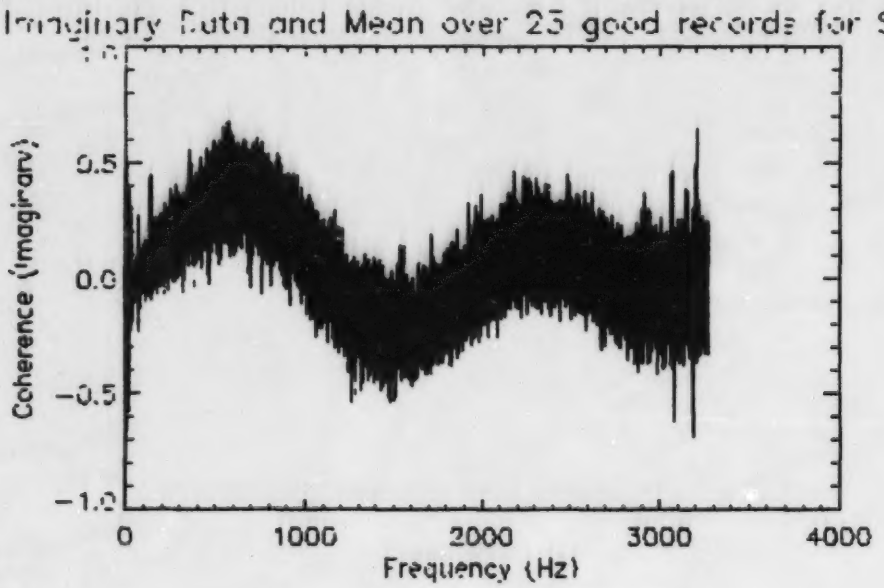

Figure 4.5. Plot of imaginary coherence as a function of frequency for the valid data records (grey) and the average data (black). Emerald Basin site, West Apex.

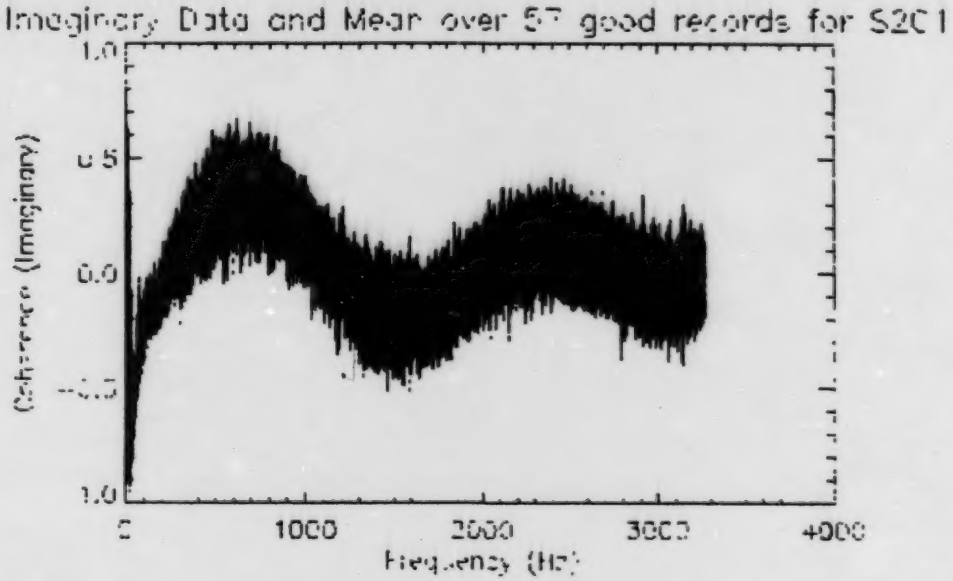


Figure 4.6. Plot of imaginary coherence as a function of frequency for the valid data records (grey) and the average data (black). Emerald Basin site, East Apex.

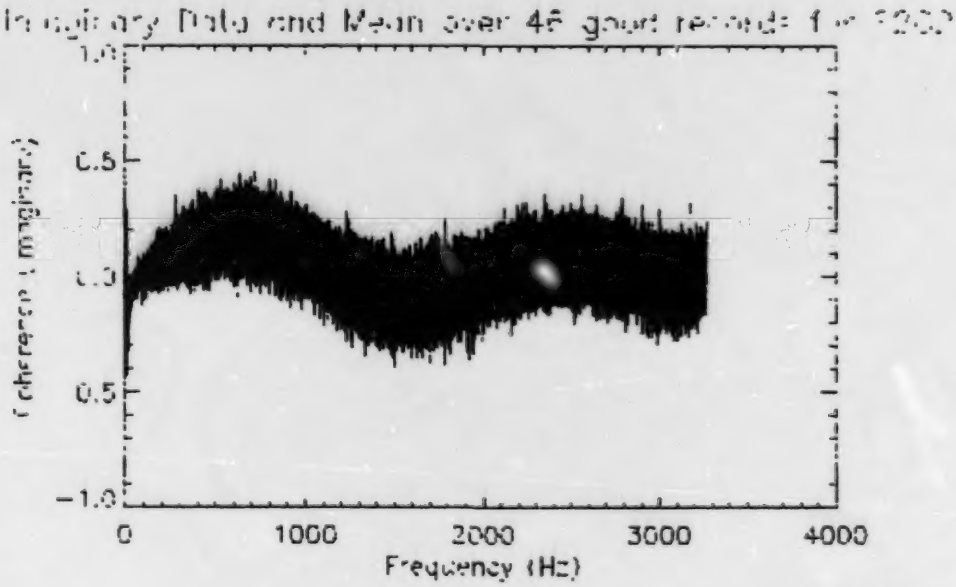

Figure 4.7. Plot of imaginary coherence as a function of frequency for the valid data records (grey) and the average data (black). North of Sable Island site, North Apex.

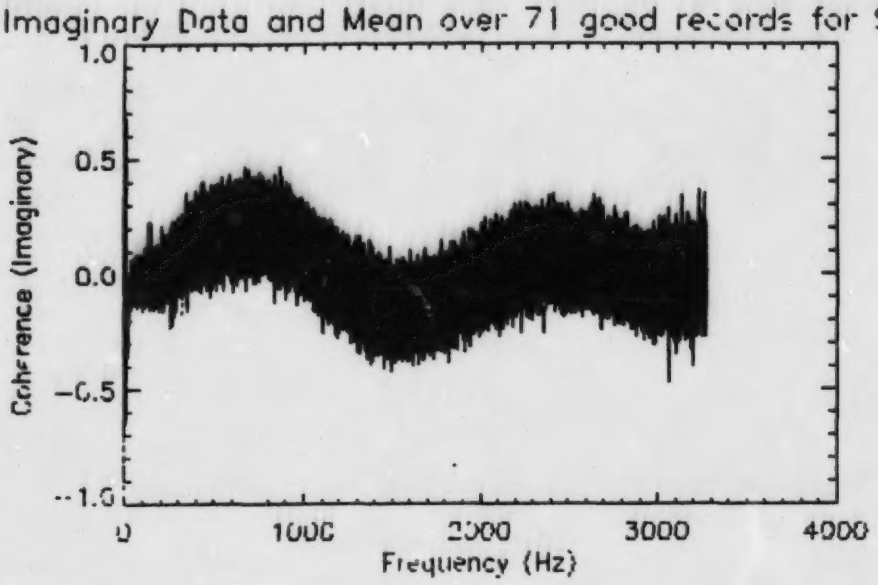


Figure 4.8. Plot of imaginary coherence as a function of frequency for the valid data records (grey) and the average data (black). North of Sable Island site, West Apex.

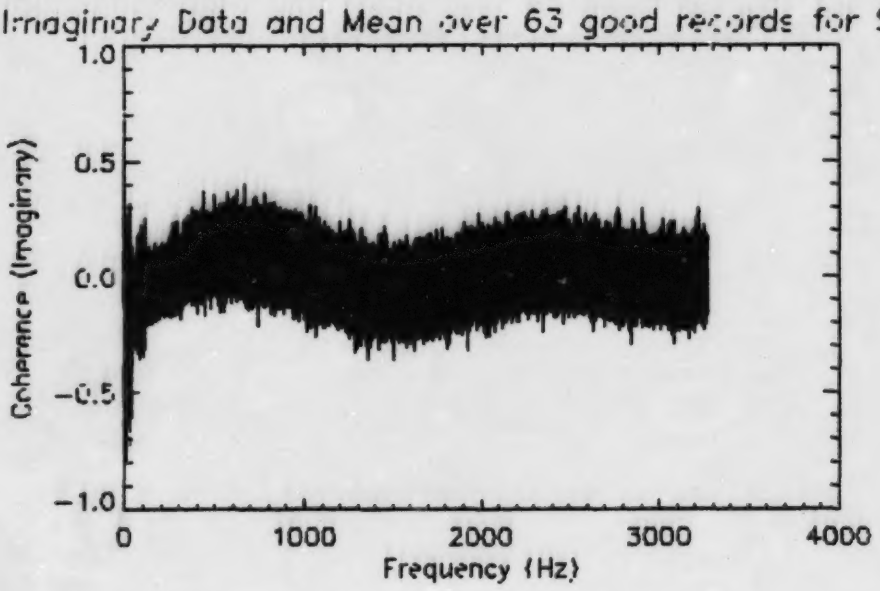

Figure 4.9. Plot of imaginary coherence as a function of frequency for the valid data records (grey) and the average data (black). Gully site, North A Apex.

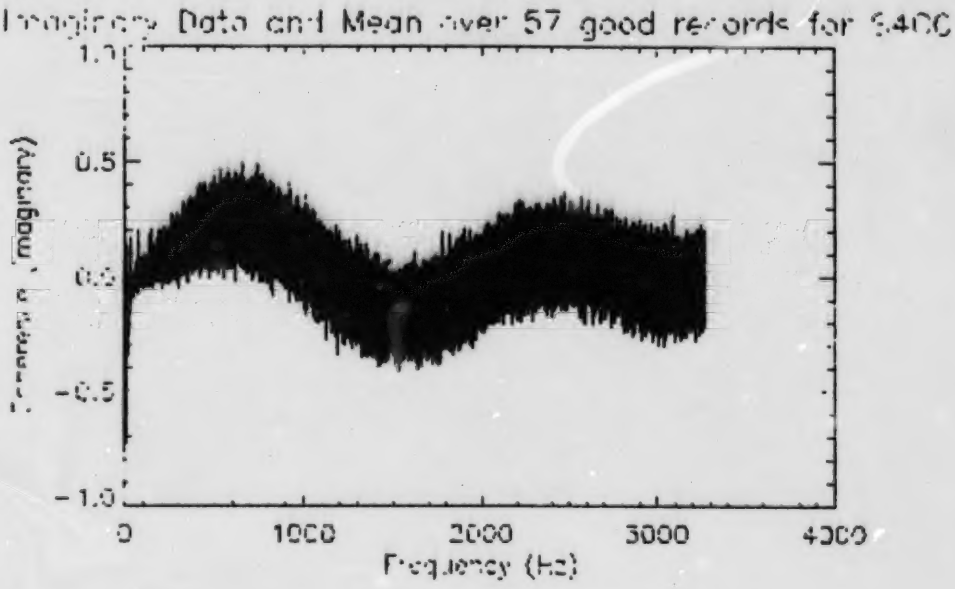


Figure 4.10. Plot of imaginary coherence as a function of frequency for the valid data records (grey) and the average data (black). Gully site, East Apex.

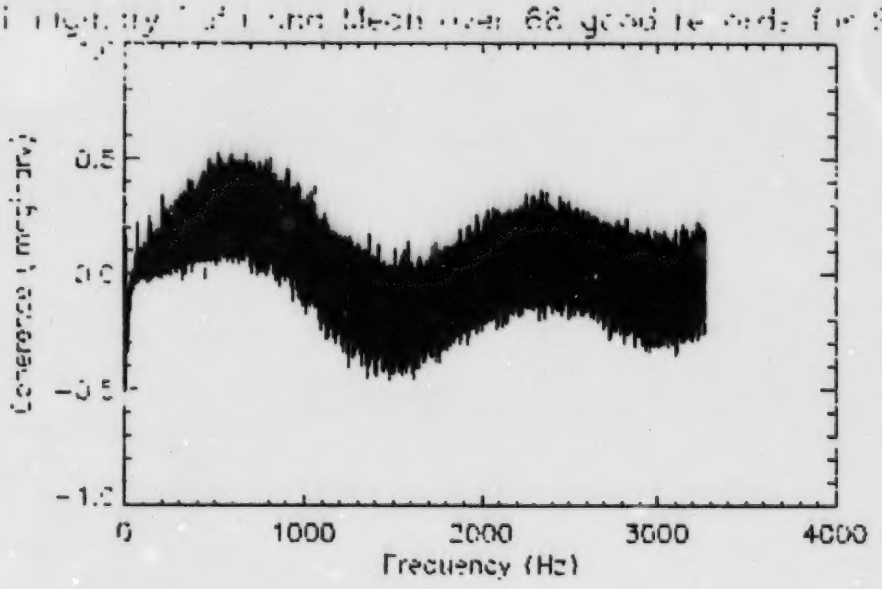

Figure 4.11. Plot of imaginary coherence as a function of frequency for the valid data records (grey) and the average data (black). Gully site, West Apex.

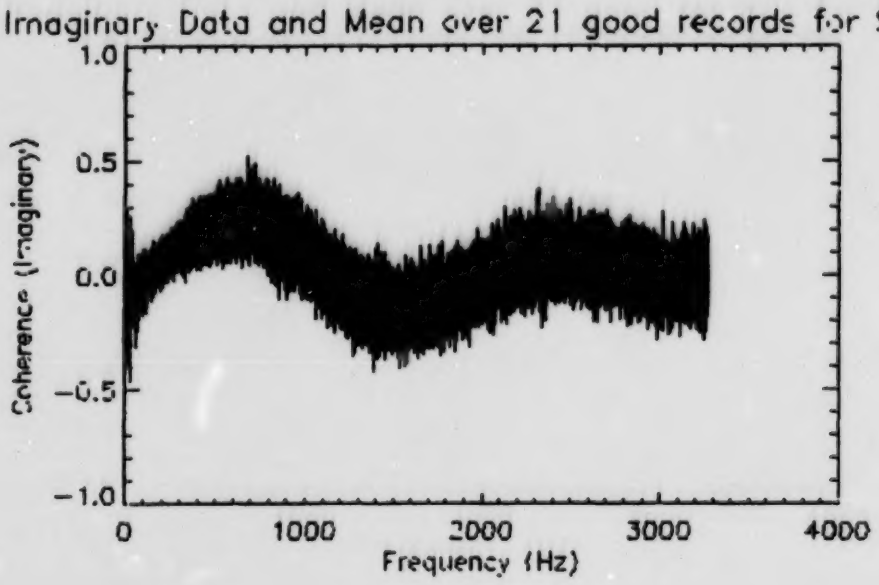


Figure 4.12. Plot of imaginary coherence as a function of frequency for the valid data records (grey) and the average data (black). Laurentian Channel site, North Apex.

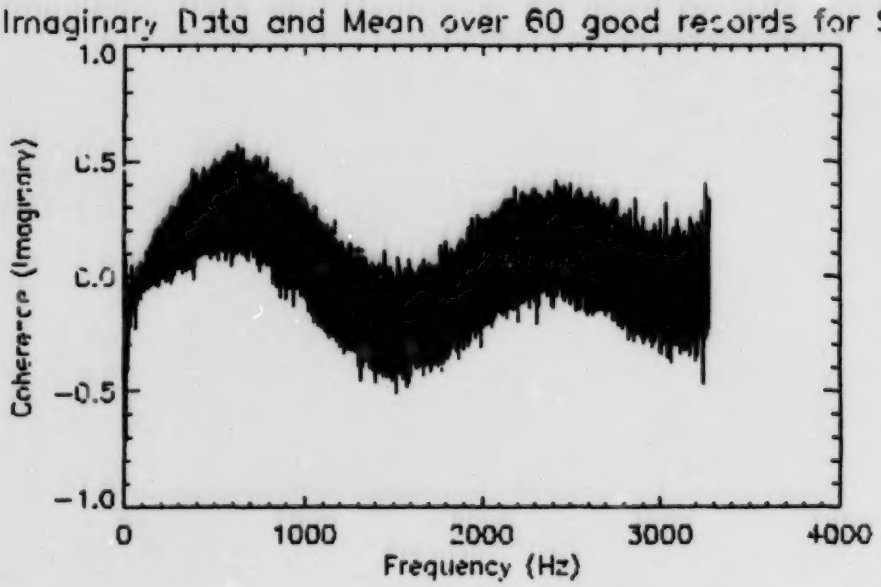

**Figure 4.13. Plot of imaginary coherence as a function of frequency for the valid data records (grey) and the average data (black). Laurentian Channel site, West Apex.**

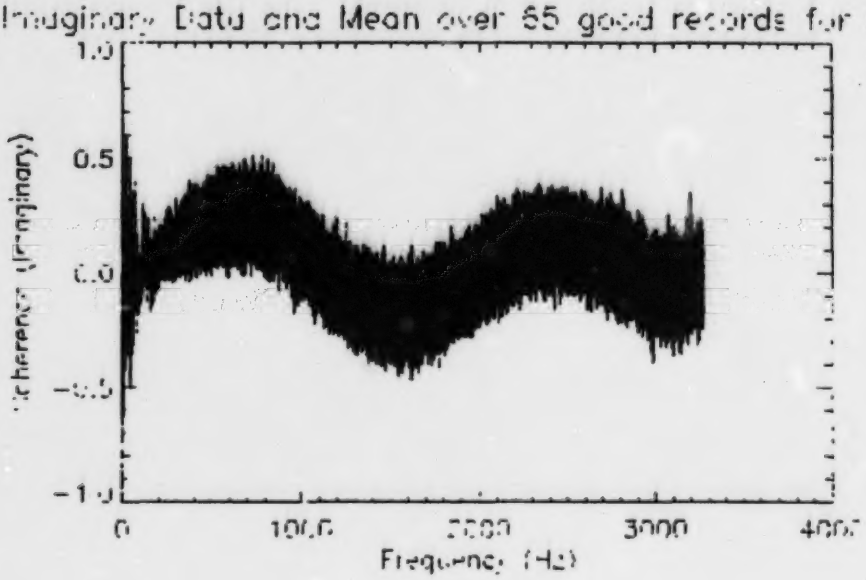

**Appendix 5.** Plots of 11-point running average of mean real coherence data.

Figure 5.1. Plot of 11-point running average of mean real coherence as a function of frequency for the valid data records of South East of Halifax site, North Apex (black) and Emerald Basin site, North Apex (grey).

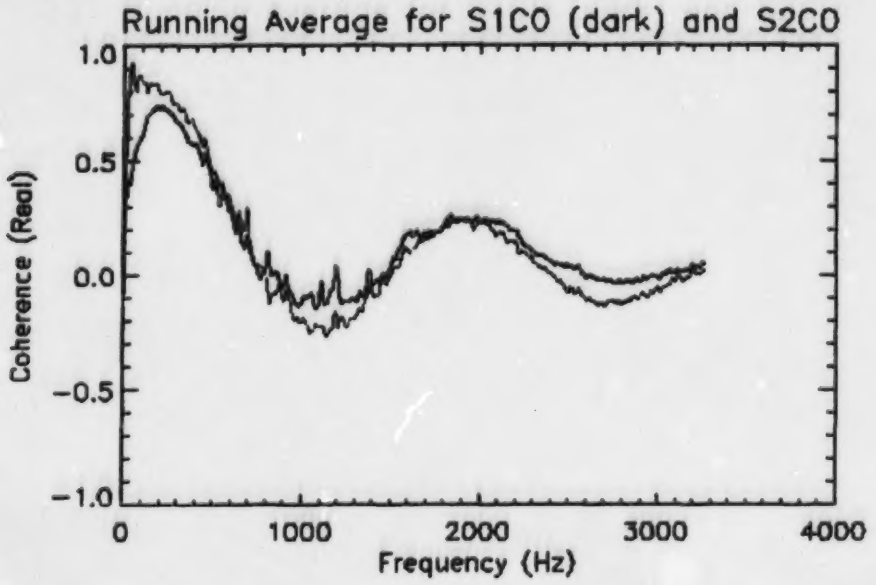


Figure 5.2. Plot of 11-point running average of mean real coherence as a function of frequency for the valid data records of South East of Halifax site (black), North Apex and North of Sable Island site, West Apex (grey).

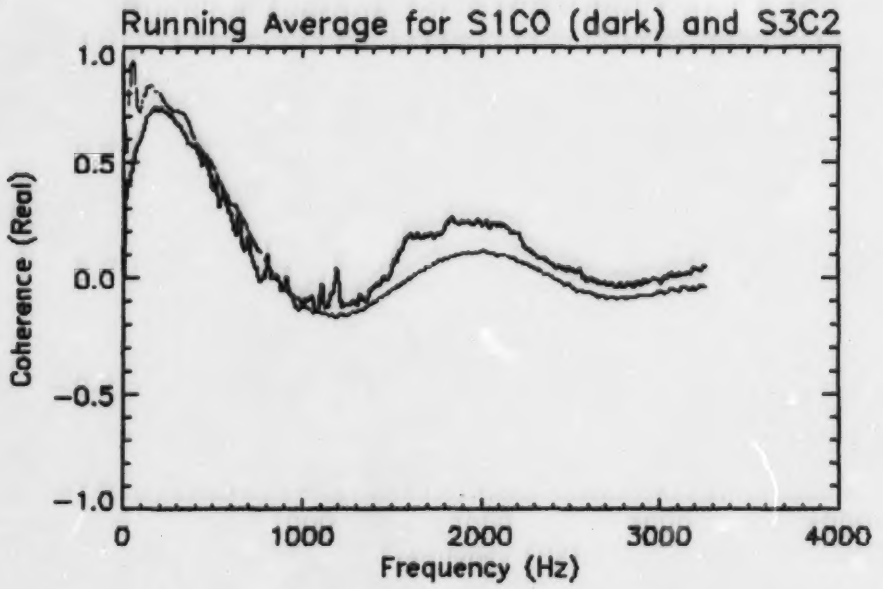

Figure 5.3. Plot of 11-point running average of mean real coherence as a function of frequency for the valid data recordsof South East of Halifax site, North Apex and Gully site, East Apex (grey).

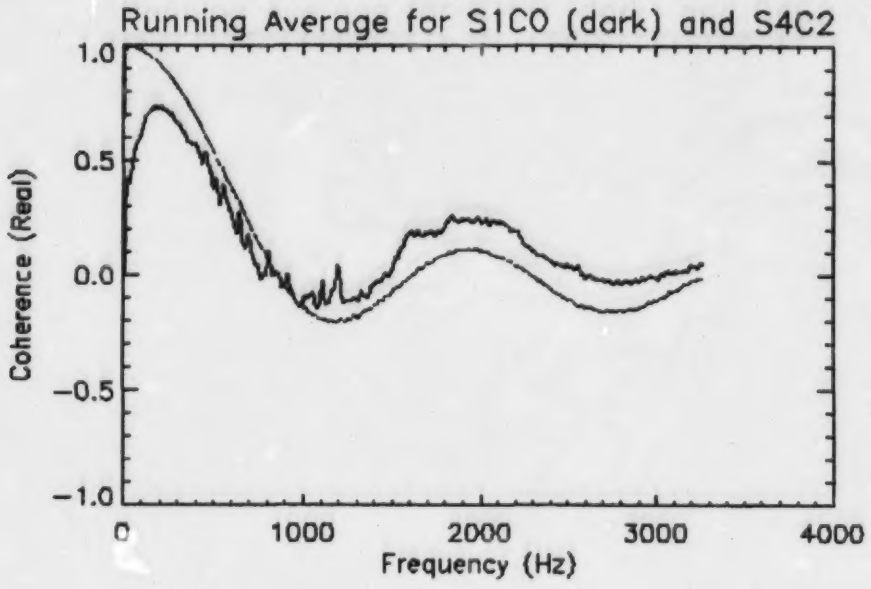


Figure 5.4. Plot of 11-point running average of mean real coherence as a function of frequency for the valid data records of South East of Halifax site, North Apex (black) and Laurentian Channel site, North Apex (grey).

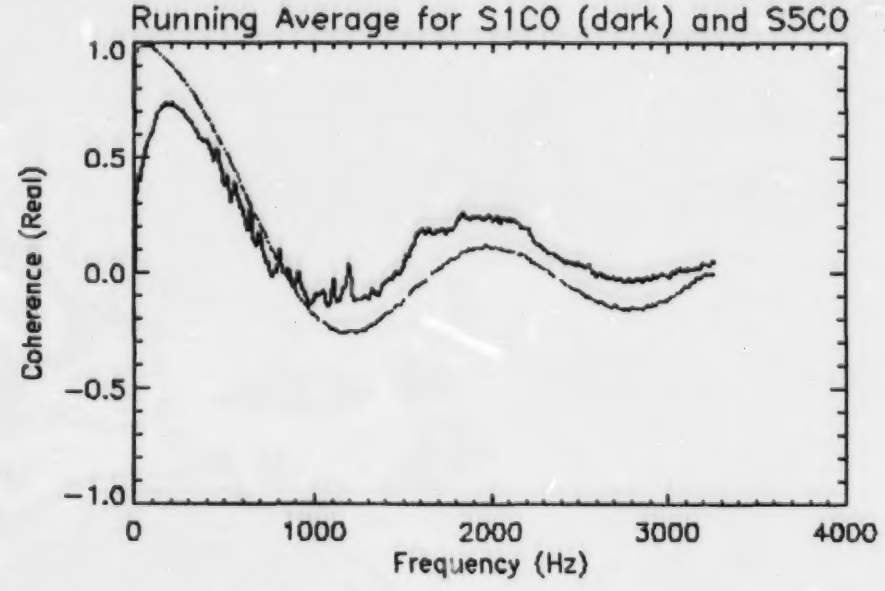

Figure 5.5. Plot of 11-point running average of mean real coherence as a function of frequency for the valid data records of Emerald Basin site, North Apex (black) and North of Sable Island site, West Apex (grey).

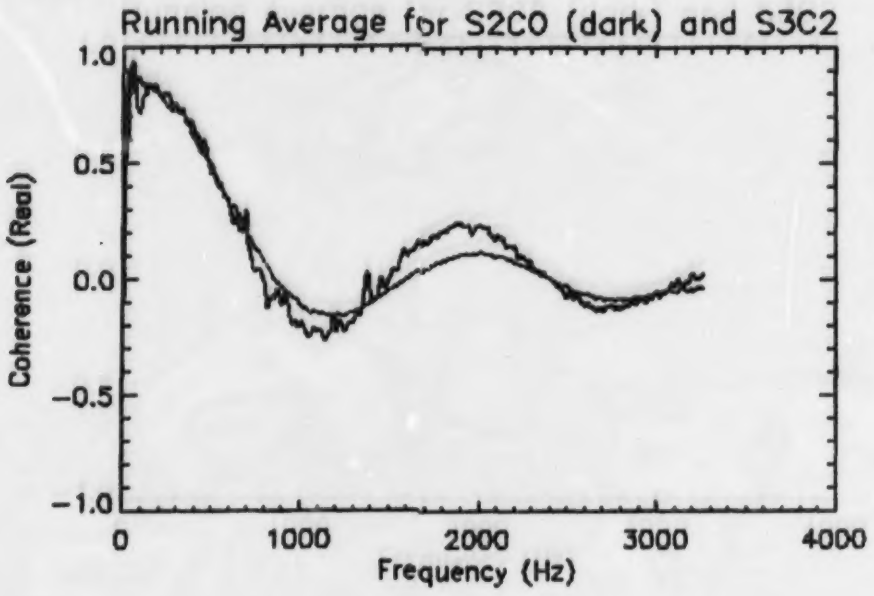


Figure 5.6. Plot of 11-point running average of mean real coherence as a function of frequency for the valid data records of Emerald Basin site, North Apex (black) and Gully site, East Apex (grey).

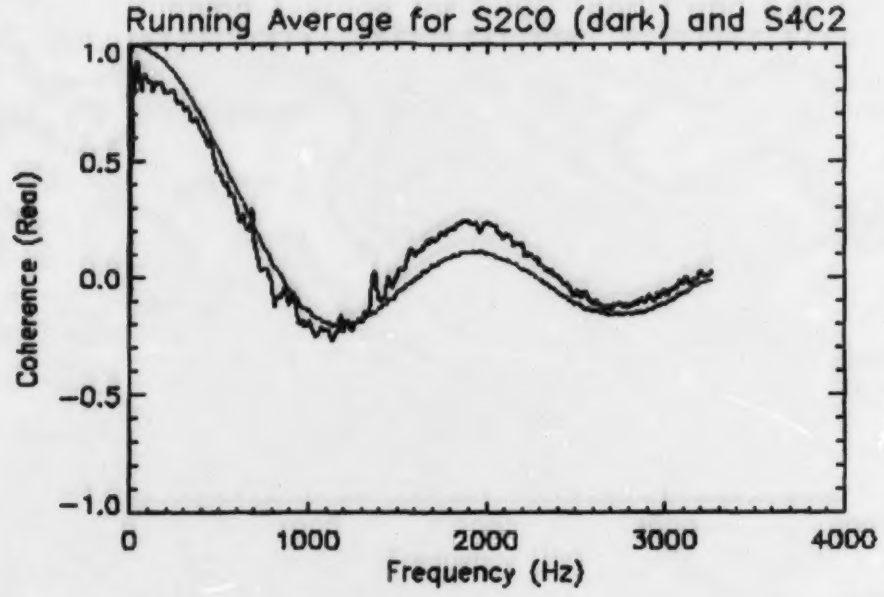

Figure 5.7. Plot of 11-point running average of mean real coherence as a function of frequency for the valid data records of Emerald Basin site, North Apex (black) and Laurentian Channel site, North Apex (grey).

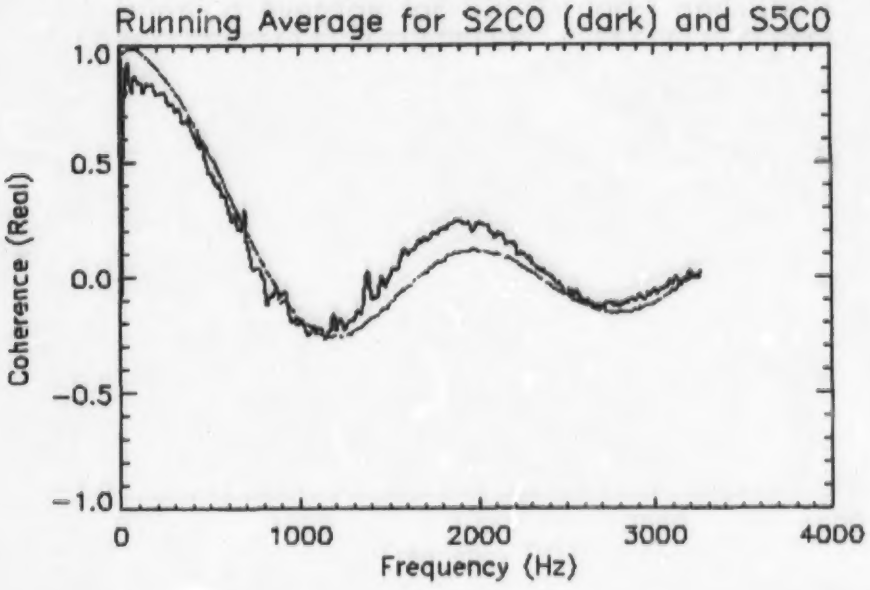


Figure 5.8. Plot of 11-point running average of mean real coherence as a function of frequency for the valid data records of North of Sable Island site, West Apex (black) and Gully site, East Apex (grey).

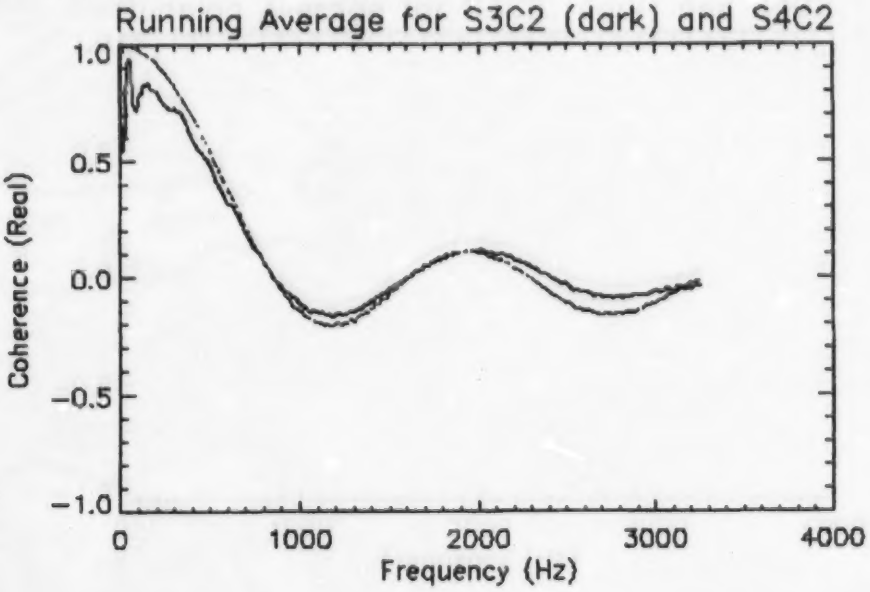

Figure 5.9. Plot of 11-point running average of mean real coherence as a function of frequency for the valid data records of North of Sable Island site, West Apex (black) and Laurentian Channel site, North Apex (grey).

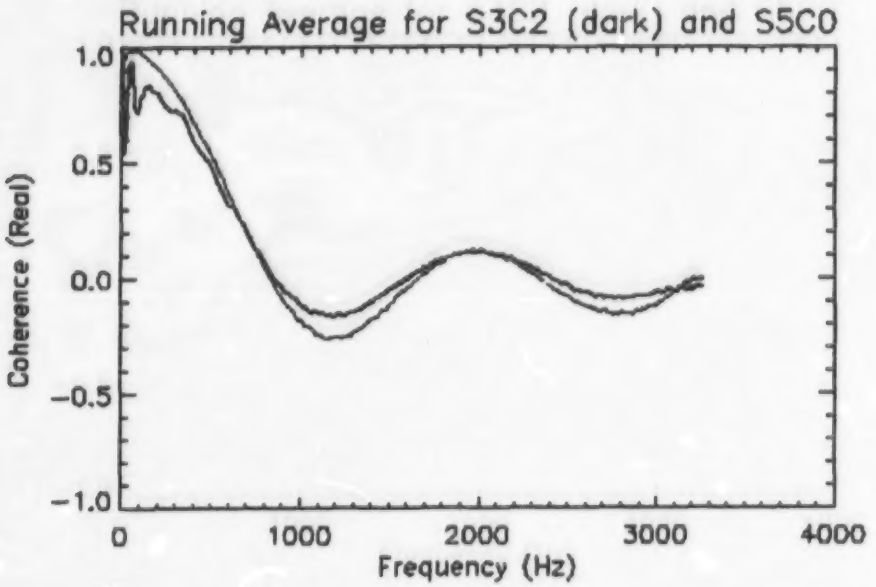


Figure 5.10. Plot of 11-point running average of mean real coherence as a function of frequency for the valid data records of Gully site, East Apex (black) and Laurentian Channel site, North Apex (grey).

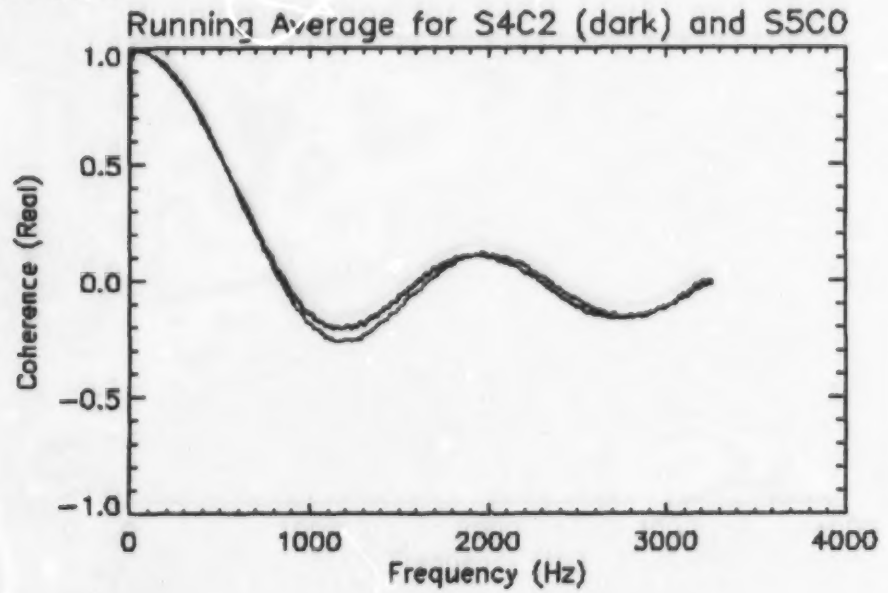

**Appendix 6.** Plots of 11-point running average of mean imaginary coherence data

Figure 6.1. Plot of 11-point running average of mean imaginary coherence as a function of frequency for the valid data records of South East of Halifax site, North Apex (black) and Emerald Basin site, North Apex (grey).

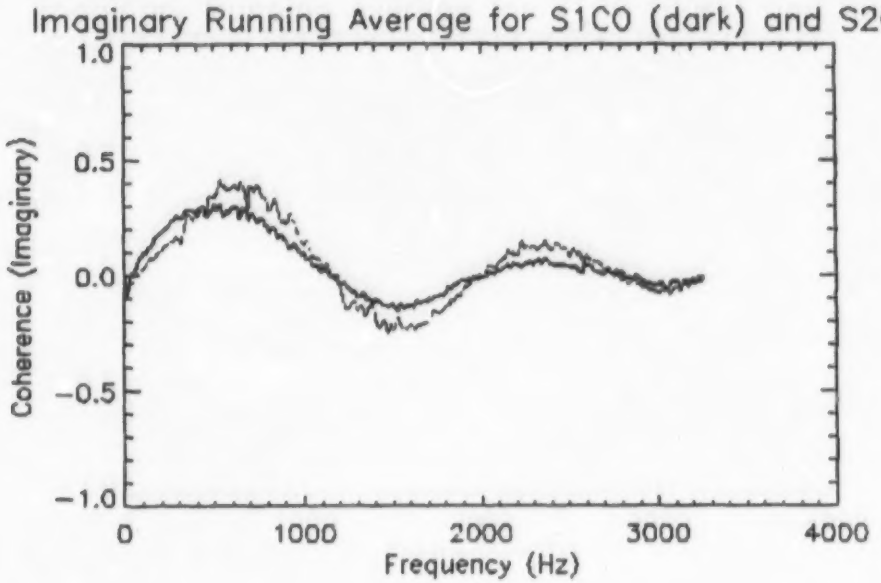


Figure 6.2. Plot of 11-point running average of mean imaginary coherence as a function of frequency for the valid data records of South East of Halifax site, North Apex (black) and North of Sable Island site, West Apex (grey).

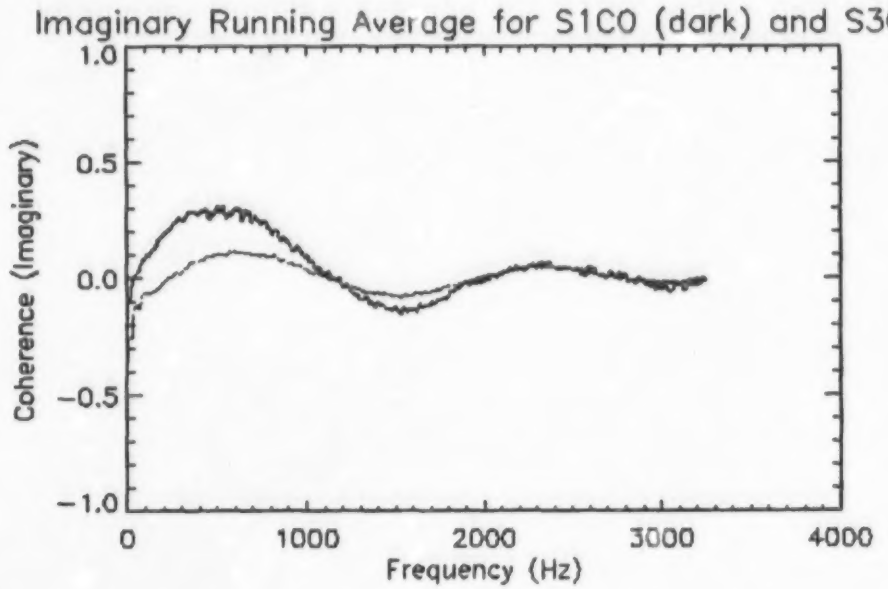

Figure 6.3. Plot of 11-point running average of mean imaginary coherence as a function of frequency for the valid data records of South East of Halifax site, North Apex (black) and Gully site, East Apex (grey).

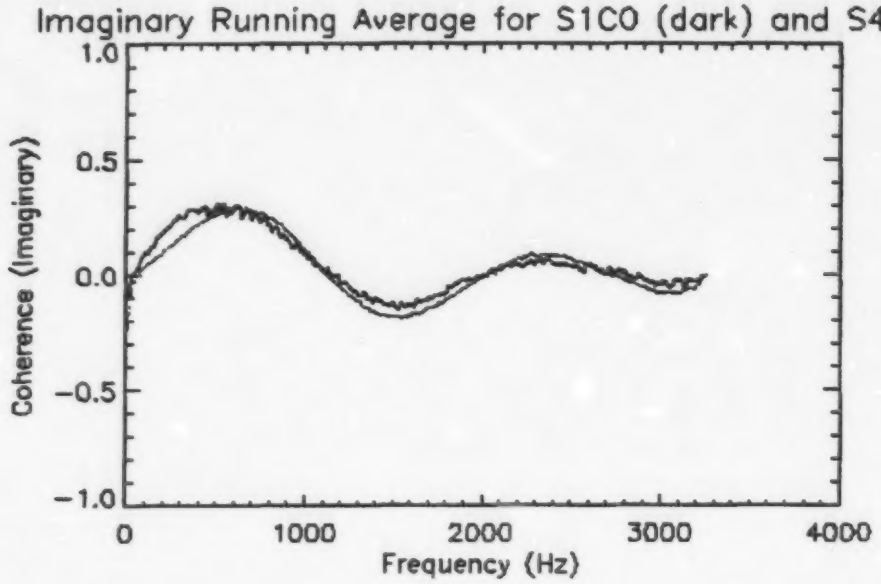


Figure 6.4. Plot of 11-point running average of mean imaginary coherence as a function of frequency for the valid data records of South East of Halifax site, North Apex (black) and Laurentian Channel site, North Apex (grey).

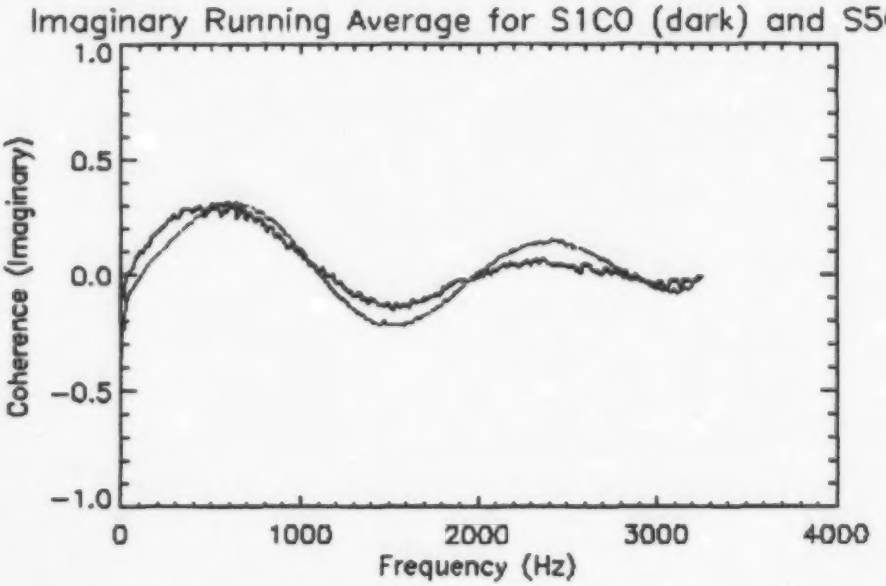

Figure 6.5. Plot of 11-point running average of mean imaginary coherence as a function of frequency for the valid data records of Emerald Basin site, North Apex (black) and North of Sable Island site, West Apex (grey).

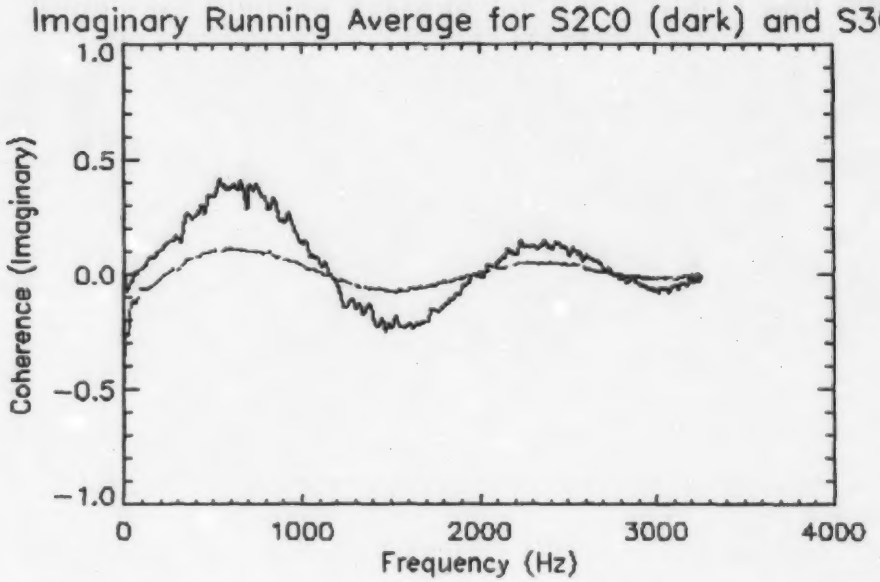


Figure 6.6. Plot of 11-point running average of mean imaginary coherence as a function of frequency for the valid data records of Emerald Basin site, North Apex (black) and Gully site, East Apex (grey).

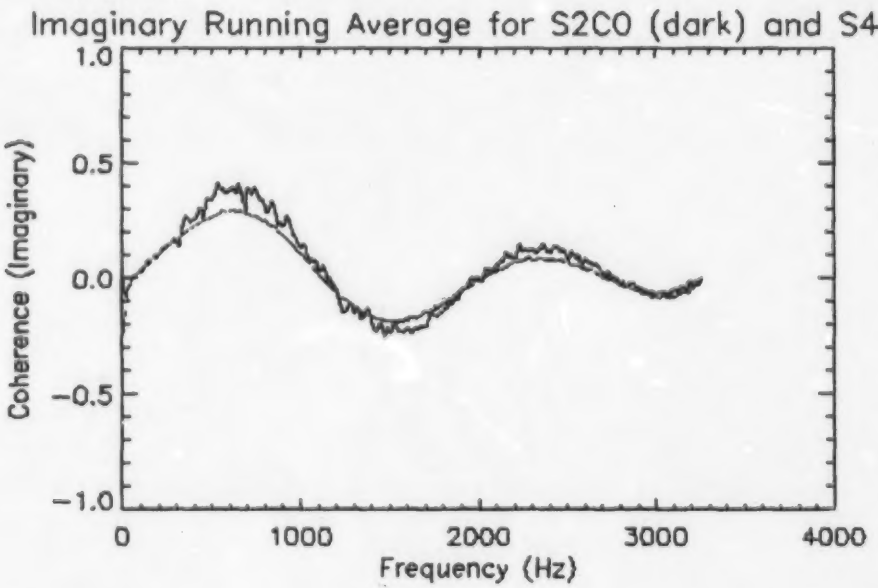

Figure 6.7. Plot of 11-point running average of mean imaginary coherence as a function of frequency for the valid data records of Emerald Basin site, North Apex and S5C0 = Laurentian Channel site, North Apex.

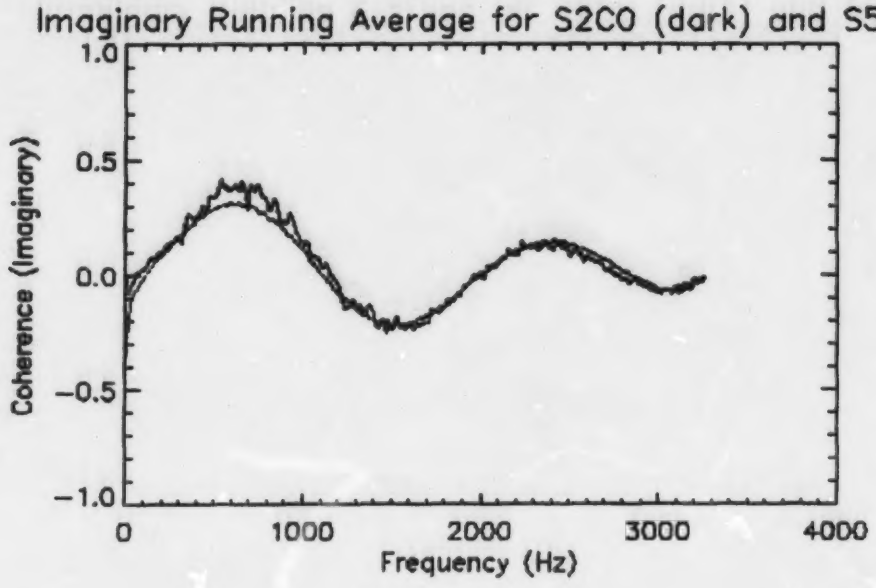


Figure 6.8. Plot of 11-point running average of mean imaginary coherence as a function of frequency for the valid data records of North of Sable Island site, West Apex (black) and Gully site, East Apex (grey).

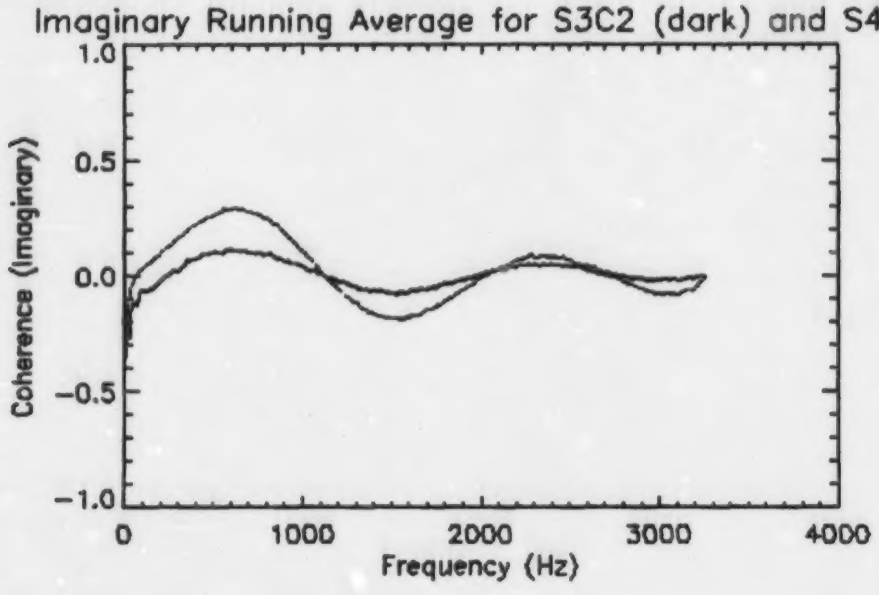

Figure 6.9. Plot of 11-point running average of mean imaginary coherence as a function of frequency for the valid data records of North of Sable Island site, West Apex (black) and Laurentian Channel site, North Apex (grey).

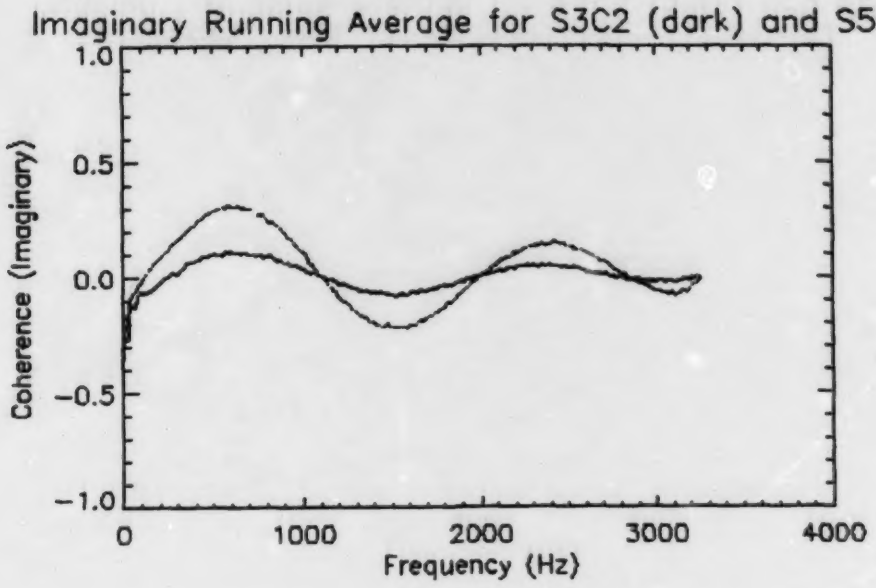


Figure 6.10. Plot of 11-point running average of mean imaginary coherence as a function of frequency for the valid data records of Gully site, East Apex (black) and Laurentian Channel site. North Apex (grey).

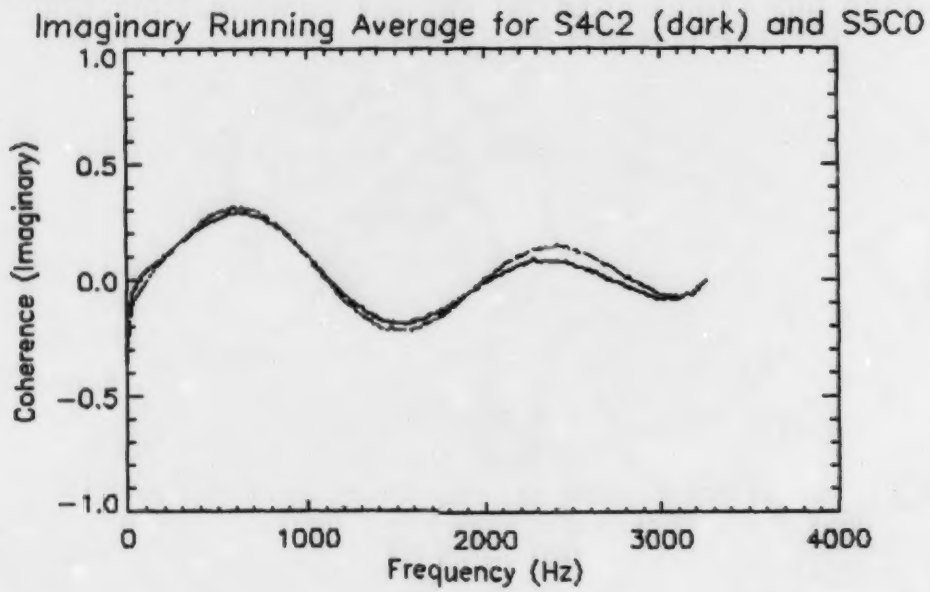

UNCLASSIFIED
SECURITY CLASSIFICATION OF FORM
(highest classification of Title, Abstract, Keywords)

**DOCUMENT CONTROL DATA**

(Security classification of title, body of abstract and indexing annotation must be entered when the overall document is classified)

1 ORIGINATOR (the name and address of the organization preparing the document Organizations for whom the document was prepared, e g Establishment sponsoring a contractor's report or tasking agency, are entered in section 8 )

Dalhousie University, Department of Oceanography

2. SECURITY CLASSIFICATION (overall security classification of the document including special warning terms if applicable)

UNCLASSIFIED

3 TITLE (the complete document title as indicated on the title page Its classification should be indicated by the appropriate abbreviation (S,C,R or U) in parentheses after the title)

Analysis of vertical noise coherence data from the EC-VNCI data set

4 AUTHORS (Last name, first name, middle initial If military, show rank, e g Doe, Maj John E )

Cory Weatherbee

| 5 DATE OF PUBLICATION (month and year of publication of document) | 6a NO OF PAGES (total containing information Include Annexes, Appendices, etc) | 6b NO OF REFS (total cited in document) |
|---|---|---|
| March 2000 | 38 (approx.) | 7 |

7 DESCRIPTIVE NOTES (the category of the document, e g technical report, technical note or memorandum If appropriate, enter the type of report e g interim, progress, summary, annual or final Give the inclusive dates when a specific reporting period is covered)

CONTRACTOR REPORT

8 SPONSORING ACTIVITY (the name of the department project office or laboratory sponsoring the research and development Include address)

Defence Research Establishment Atlantic
PO Box 1012, Dartmouth, NS, Canada B2Y 3Z7

| 9a PROJECT OR GRANT NO (if appropriate the applicable research and development project or grant number under which the document was written Please specify whether project or grant) | 9b CONTRACT NO (if appropriate, the applicable number under which the document was written) |
|---|---|
| Project 1ca11 | W7707-9-6918 |

| 10a ORIGINATOR'S DOCUMENT NUMBER (the official document number by which the document is identified by the originating activity This number must be unique to this document ) | 10b OTHER DOCUMENT NOs (Any other numbers which may be assigned this document either by the originator or by the sponsor ) |
|---|---|
| | DREA CR 2000-030 |

11 DOCUMENT AVAILABILITY (any limitations on further dissemination of the document, other than those imposed by security classification)

( X ) Unlimited distribution
( ) Defence departments and defence contractors; further distribution only as approved
( ) Defence departments and Canadian defence contractors; further distribution only as approved
( ) Government departments and agencies; further distribution only as approved
( ) Defence departments; further distribution only as approved
( ) Other (please specify):

12 DOCUMENT ANNOUNCEMENT (any limitation to the bibliographic announcement of this document This will normally correspond to the Document Availability (11) However, where further distribution (beyond the audience specified in (11) is possible, a wider announcement audience may be selected)

UNCLASSIFIED
SECURITY CLASSIFICATION OF FORM

UNCLASSIFIED
SECURITY CLASSIFICATION OF FORM
*(highest classification of Title, Abstract, Keywords)*

13. ABSTRACT (a brief and factual summary of the document It may also appear elsewhere in the body of the document itself It is highly desirable that the abstract of classified documents be unclassified Each paragraph of the abstract shall begin with an indication of the security classification of the information in the paragraph (unless the document itself is unclassified) represented as (S), (C), (R), or (U) It is not necessary to include here abstracts in both official languages unless the text is bilingual)

In a shallow water environment, some physical properties of the surficial sediments, such as the compressional and shear speed, can be inverted from ambient noise data. Vertical noise coherence data were collected over five sites on the Scotian Shelf and Laurentian Channel. The sites were chosen because of their various sediment properties, in order to quantify whether the differences in vertical coherence would allow differentiation among sediment types. It was found that some sediment types could be differentiated using either the real or imaginary part of the vertical noise coherence (e.g. Sable Island gravel from LaHave clay), while others showed coherence results that were too similar to be differentiated using this technique (e.g. Scotian Shelf drift and LaHave clay). Sites with shipping noise contamination can be difficult to classify.

14 KEYWORDS, DESCRIPTORS or IDENTIFIERS (technically meaningful terms or short phrases that characterize a document and could be helpful in cataloguing the document They should be selected so that no security classification is required Identifiers, such as equipment model designation, trade name, military project code name, geographic location may also be included If possible keywords should be selected from a published thesaurus e g Thesaurus of Engineering and Scientific Terms (TEST) and that thesaurus-identified If it not possible to select indexing terms which are Unclassified, the classification of each should be indicated as with the title)

Vertical noise coherence
Scotian Shelf
Laurentian Channel
Inversion

UNCLASSIFIED
SECURITY CLASSIFICATION OF FORM